2017

ANALYTICAL AND BOUNDARY ELEMENT SOLUTIONS OF BULK REACTING LINED DUCTS AND PARALLEL-BAFFLE SILENCERS

Jundong Li
University of Kentucky, usjundong@gmail.com
Author ORCID Identifier:
https://orcid.org/0000-0003-3891-6957
Digital Object Identifier: https://doi.org/10.13023/ETD.2017.348

STUDENT AGREEMENT:

I represent that my thesis or dissertation and abstract are my original work. Proper attribution has been given to all outside sources. I understand that I am solely responsible for obtaining any needed copyright permissions. I have obtained needed written permission statement(s) from the owner(s) of each third-party copyrighted matter to be included in my work, allowing electronic distribution (if such use is not permitted by the fair use doctrine) which will be submitted to UKnowledge as Additional File.

I hereby grant to The University of Kentucky and its agents the irrevocable, non-exclusive, and royalty-free license to archive and make accessible my work in whole or in part in all forms of media, now or hereafter known. I agree that the document mentioned above may be made available immediately for worldwide access unless an embargo applies.

I retain all other ownership rights to the copyright of my work. I also retain the right to use in future works (such as articles or books) all or part of my work. I understand that I am free to register the copyright to my work.

REVIEW, APPROVAL AND ACCEPTANCE

The document mentioned above has been reviewed and accepted by the student's advisor, on behalf of the advisory committee, and by the Director of Graduate Studies (DGS), on behalf of the program; we verify that this is the final, approved version of the student's thesis including all changes required by the advisory committee. The undersigned agree to abide by the statements above.

Jundong Li, Student

Dr. Tingwen Wu, Major Professor

Dr. Haluk E. Karaca, Director of Graduate Studies

ANALYTICAL AND BOUNDARY ELEMENT SOLUTIONS OF BULK-REACTING LINED DUCTS AND PARALLEL-BAFFLE SILENCERS

THESIS

A Thesis submitted in partial fulfillment of the
requirements for the degree of Master of Science
in Mechanical Engineering in the College of Engineering
at the University of Kentucky

By

Jundong Li

Lexington, Kentucky

Director: Dr. Tingwen Wu, Professor of Mechanical Engineering

Co-Director: Dr. David W. Herrin, Professor of Mechanical Engineering

Lexington, Kentucky

2017

ABSTRACT OF THESIS

ANALYTICAL AND BOUNDARY ELEMENT SOLUTIONS OF BULK-REACTING LINED DUCTS AND PARALLEL-BAFFLE SILENCERS

Lined silencers of various configurations are used to attenuate the noise from building HVAC equipment, gas turbines, and other machinery. First-mode analytical solutions are presented for sound attenuation along rectangular lined ducts, parallel-baffle silencers, and circular lined ducts. The sound absorptive lining is treated using a bulk property model. The analytical solutions entail solving a nonlinear characteristic equation in the transverse direction after the rigid-wall boundary condition is applied. The solution is compared to the boundary element solution and a local impedance analytical solution for several test cases.

KEYWORDS: Boundary Element Method, Lined Duct, Parallel-Baffle Silencer, Transmission Loss, Dissipative Silencer

Jundong Li

20th July 2017

ANALYTICAL AND BOUNDARY ELEMENT SOLUTIONS OF BULK-REACTING LINED DUCTS AND PARALLEL-BAFFLE SILENCERS

By

Jundong Li

Dr. Tingwen Wu
Director of Thesis

Dr. David W. Herrin
Co-Director of Thesis

Dr. Haluk E. Karaca
Director of Graduate Studies

20th July, 2017
Date

To my parents, Guijun Li and Min Xie, and my beloved wife, Chan Dai.

ACKNOWLEDGEMENTS

Foremost, I would like to express my special appreciation and thanks to my advisor Professor Tingwen Wu and for his continuous guidance and patience during both my undergraduate and graduate studies at the University of Kentucky. He has been a tremendous mentor for me. I do appreciate my co-advisor Professor David W. Herrin as well for his help and advice during my studies. I am also grateful to both of them for offering me the opportunities to participate in training and conderences and providing me with exprosure to excitingly diverse industrial projects.

My sincere thanks also go to Dr. John Baker for providing great help and valuable advice on my research.

I would like to thank my fellows and friends in the Vibro-Acoustics group: Wanlu Li, Huangxing Chen, Shujian He, Gong Cheng, Yitian Zhang, Kangping Ruan, Keyu Chen, Peng Wang, Ruimeng Wu, Weiyun Liu, Shishuo Sun, Caoyang Li, Nan Zhang, Jonathan Chen, Xin Hua, Limin Zhou, Jinghao Liu, Jiawei Liu, and Rui He, for all the fun we have had in the past several years, and for every priceless effort they have made to help me on career development.

I also want to express my special thanks to my family. Words cannot express how grateful I am to my mother Min Xie and my father Guijun Li for all of the sacrifices that they have made on my behalf. Your prayer for me was what sustained me thus far. A very special acknowledgement goes to my beloved wife

Chan Dai, who loved and spiritually supported me, and made me feel like anything was possible during my graduate study.

TABLE OF CONTENTS

LIST OF FIGURES

CHAPTER 1 INTRODUCTION

1.1 Introduction

In order to meet regulations and to provide greater customer satisfaction, industry is investing in efforts to reduce noise from their products. Lined ducts and parallel-baffle silencers are widely used to guide exhaust gas and to dissipate sound from large equipment and power plants. Common locations include insertion into HVAC (heating, ventilation, and air conditioning) ductwork, openings of large enclosures for power generating equipment, silencers for large engines, and ducted outlets of gas turbines and power plant cooling towers.

In general, there are two widely used approaches for modeling dissipative silencers. For cases that require higher accuracy, engineers generally use numerical simulation including the finite element (FEM) and boundary element methods (BEM) [4, 5]. For conceptual design purposes, engineers prefer analytical solutions so that the effect of design changes ca be assessed without the need for meshing or long model solution times. Sometimes, experimental methods may also be used to validate analytical or numerical methods. For simplicity, most analytical approaches use locally reacting method to model sound absorptive lining where the surface of the liner is modeled as a surface impedance. Wave propagation through the absorber is not accounted for.

In 1939, Morse [6] developed equations for sound transmission inside pipes with dimensions large enough to neglect the effect of viscosity. In that publication,

he developed formulas to calculate sound pressure, particle velocity and sound attenuation in pipes assuming a locally reacting assumption. Design graphs were provided for quick prediction of sound attenuation. Theories of sound transmission assuming a locally reacting liner have been studied by several other researchers with certain success. In 1994, Ingard [7] presented a series of analytical solutions including the first cut-on mode for sound attenuation along the longitudinal direction of various lined ducts using the locally reacting approach.

In 1946, Scott [8] looked at the limitations of the locally reacting model and developed the more complicated bulk-reacting approach. In Scott's analysis, he solved the lined duct problem by assuming a separate acoustic wave inside the sound absorbing material. He also compared the results with available experimental data as well as Morse's [6] locally reacting model and discovered that a locally reacting model was inaccurate at higher frequencies whereas a bulk reacting model is satisfactory. For rectangular lined ducts, Scott modeled the duct in two-dimensions and hence only included sound absorption on two sides of the duct.

Several measurement studies have been performed in the literature. In 1948, Brittain et al. [9] developed experimental curves of sound attenuation for various duct sizes and different thickness liners. Later, King [10] provided additional experimental curves for larger ducts and thicker sound absorptive linings.

1.2 Motivation and Objective

Although the numerical methods, such as the FEM and BEM, can provide more accurate predictions than any of the approximate analytical methods, and can handle complex geometry, they do require building a 3D mesh first, which is labor intensive, and the numerical analysis itself at high frequencies can also be very time consuming.

In industry, it is critical to have a rapid design tool to permit noise engineers to predict sound attenuation of a specific design before building a numerical simulation model in three-dimensions. The objective of this thesis is to develop a set of 2D and 3D bulk-reacting analytical methods to predict sound attenuation in parallel-baffle silencers as well as circular and rectangular lined ducts. Frequencies above the first cut-off or transverse mode of the duct are included.

The proposed methods are based on the same first-mode analytical methods developed by Ingard [7] except that the bulk-reacting assumption is now used instead of Ingard's locally reacting assumption. Bulk-reacting results are compared to the locally reacting results as well as the full 3D BEM results.

1.3 Thesis Organization

This chapter briefly introduces the proposed work and includes a brief literature review. The motivation and objectives for the research are discussed.

Chapter 2 presents the theoretical background and details the approach for the research.

Chapter 3 details the methodology for the locally reacting and bulk reacting analytical approaches.

Chapter 4 includes validation studies for the proposed methods as well as discussions on the results.

Chapter 5 concludes the thesis by summarizing the contributions and important outcomes, and includes suggestions for future research.

CHAPTER 2 BACKGROUND

2.1 Background

2.1.1 Linear Acoustics in the Frequency Domain

The governing differential equation for linear acoustics in the frequency domain is the famous Helmholtz equation:

$$\nabla^2 p + k^2 p = 0 \tag{2-1}$$

where p is the sound pressure and k is the wavenumber defined by

$$k = \frac{\omega}{c} \tag{2-2}$$

in which ω is the circular frequency in rad/s and c is the speed of sound.

For waves traveling only in the x direction, the general one-dimensional solution to Eq. (2-1) is：

$$p = Ae^{-ikx} + Be^{ikx} \tag{2-3}$$

alternatively, in sinusoidal form:

$$p = A\cos(kx) + B\sin(kx) \tag{2-4}$$

The particle velocity can be derived from the momentum equation and the result is:

$$u_x = \frac{i}{\rho_0 \omega}\frac{dp}{dx} = \frac{1}{\rho_0 c}(Ae^{-ikx} - Be^{+ikx}) \qquad (2\text{-}5)$$

alternatively, in a sinusoidal form:

$$u_x = \frac{i}{\rho_0 \omega}\frac{dp}{dx} = \frac{i}{\rho_0 c}[A\sin(kx) + B\cos(kx)] \qquad (2\text{-}6)$$

Equations 2-3 through 2-6 are the solutions for one-dimensional sound propagation in a duct assuming that the cross-sectional area stays the same. As such, these equations are only valid up to the cut-off frequency which occurs as the first transverse mode. For a rectangular duct, the cutoff frequency occurs at $\frac{c}{2d}$ where d is the largest duct dimension. For a circular duct, the first transverse mode occurs at $\frac{c}{1.81d}$ where d is the duct diameter.

2.1.2 Transmission Loss and Sound Attenuation

Transmission loss (TL) is an important muffler performance parameter, and is defined as the difference between the incident and transmitted sound power levels in decibels assuming that the termination is anechoic.

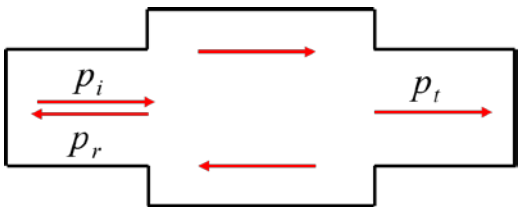

Figure 2.1 Definition of Transmission Loss

With reference to Figure 2.1, let p_i denote the incident sound pressure, p_r denotes the reflected sound pressure, and p_t denotes the transmitted sound pressure. Transmission loss (TL) in dB is defined as:

$$TL = 10\log_{10}\frac{|p_i|^2 S_1}{|p_t|^2 S_2} \tag{2-7}$$

where S_1 is the area of inlet and S_2 is the area of outlet

For large dissipative silencers, there is little reflected sound since most of the sound energy either is absorbed by the sound absorbing materials or is transmitted down the duct. Therefore, a simpler performance index called sound attenuation or noise reduction [1] is often used as an alternative to TL:

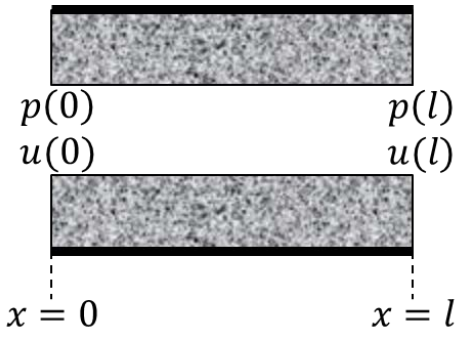

Figure 2.2 Definition of Sound Attenuation

$$Attenuation = 20\log_{10}\frac{|p(0)|}{|p(l)|} \tag{2-8}$$

With reference to Figure 2.2, $p(0)$ and $u(0)$ denote the sound pressure and the particle velocity at $x = 0$, and $p(l)$ and $u(l)$ denote the corresponding sound

pressure and the particle velocity at $x = l$. For large dissipative silencers, sound attenuation is almost identical to the TL.

2.1.3 Four-pole Transfer Matrix

The four-pole transfer matrix is a convenient tool for one-dimensional analysis in acoustics. This matrix relates the sound pressure and particle velocity at two points in a muffler element.

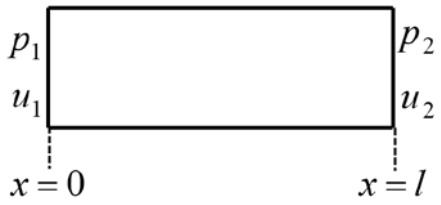

Figure 2.3 Definition of Four-Pole Transfer Matrix

For a straight duct without any lining as shown in Figure 2.3, the four-pole transfer matrix is

$$\begin{bmatrix} p_1 \\ u_1 \end{bmatrix} = \begin{bmatrix} \cos(kl) & i\rho_0 c \sin(kl) \\ \frac{i}{\rho_0 c}\sin(kl) & \cos(kl) \end{bmatrix} \begin{bmatrix} p_2 \\ u_2 \end{bmatrix} \tag{2-9}$$

For more complex muffler elements, the four-pole matrix has to be derived by an approximate analytical solution or by a numerical method.

2.1.4 Locally Reacting Lining and Bulk-Reacting Lining

The dissipation of sound energy in large dissipative silencers is normally accomplished by adding porous linings on the wall of the silencer. When analyzing sound propagation inside a lined duct, a locally or bulk reacting lining may be assumed.

The locally reacting assumption is more common and widely used due to its simplicity. It assumes that the liner can be treated as a set of parallel capillaries perpendicular to the wall and any part of the liner is only locally reacting, which means each capillary behaves independently from any other part of the liner. The wave component within the material parallel to the surface is attenuated rapidly. The propagation of sound waves inside the liner is assumed to be only in the normal direction and can be characterized by a local impedance Z, which is defined by:

$$Z = \frac{p}{u_n} \tag{2-10}$$

where u_n is the particle velocity normal to the surface.

The bulk-reacting assumption is more complicated, but can produce a more accurate solution depending on the configuration and frequency. With this assumption, the three-dimensional sound propagation inside the liner is fully considered. The sound propagation in the liner is no longer assumed to be only in the normal direction. A complex speed of sound c^* and a complex density ρ^* are

used in the Helmholtz equation to characterize the bulk-reacting material. These two material properties can be measured by the two-cavity method [11] or the two-load method [12,13,25].

2.1.5 Local Impedance of a Lining

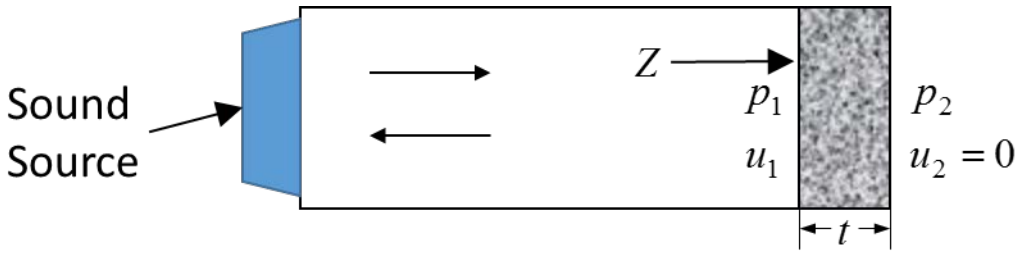

Figure 2.4 Local Impedance of a Lining

Once the two complex bulk-reacting material properties, ρ^* and c^*, are measured, the normal local impedance of a lining can be derived from the four-pole transfer matrix. With reference to Figure 2.4, the four-pole transfer matrix for the liner is:

$$\begin{Bmatrix} p_1 \\ u_1 \end{Bmatrix} = \begin{bmatrix} \cos(k^* t) & i\rho^* c^* \sin(k^* t) \\ \dfrac{i}{\rho^* c^*} \sin(k^* t) & \cos(k^* t) \end{bmatrix} \begin{Bmatrix} p_2 \\ u_2 \end{Bmatrix} \tag{2-11}$$

where k^* is the complex wavenumber, and t is the thickness of the liner. Applying the rigid-wall boundary condition, $u_2 = 0$, the local Impedance can be calculated by

$$Z = \frac{p_1}{u_1} = -i\rho^* c^* \cot\left(k^* t\right) \tag{2-12}$$

The local impedance is often normalized by the characteristic impedance ρc. In that case, normalized impedance and admittance can be expressed as the normalized impedance

$$Z_n = \frac{-i\rho^* c^* \cot\left(k^* t\right)}{\rho c} \tag{2-13}$$

and the normalized admittance

$$\eta = \frac{i\rho c \tan(k^* t)}{\rho^* c^*} \tag{2-14}$$

2.1.6 Empirical Equations for the Bulk-Reacting Material Properties

The two bulk-reacting material properties, ρ^* and c^*, can be estimated by an empirical equation if the flow resistivity is known. Although there are various empirical equations for different types of materials, most of them produce similar results. The empirical equations that follow are the well known [14, 15, 16, 17].

The characteristic Impedance of the material at room temperature, $Z_0 = \rho^* c^*$, can be calculated by

$$Z_0 = R + iX \tag{2-15}$$

$$R = \rho c\left[1 + 0.0571\left(\frac{\rho f}{R_1}\right)^{0.754}\right] \tag{2-16}$$

$$X = -\rho c\left[0.0870\left(\frac{\rho f}{R_1}\right)^{-0.732}\right] \tag{2-17}$$

where ρ is the air density in kg/m^3, c is the speed of sound in air, f is the frequency in Hz, and R_1 is the flow resistivity in Rayl/m. The propagation constant b can be calculated by

$$b = \alpha + i\beta \tag{2-18}$$

$$\alpha = \frac{\omega}{c}\left[0.189\left(\frac{\rho f}{R_1}\right)^{-0.595}\right] \tag{2-19}$$

$$\beta = \frac{\omega}{c}\left[1 + 0.0978\left(\frac{\rho f}{R_1}\right)^{-0.700}\right] \tag{2-20}$$

The complex wavenumber of the material is:

$$k^* = -i\alpha + \beta \tag{2-21}$$

The above empirical equations are accurate in the flow resistivity range of

$$0.01 \le \frac{\rho f}{R_1} \le 1 \tag{2-22}$$

At high temperature, there is also correction factor that can be applied to the equations. This is significant since very few labs in the world have the capability to measure the sound absorption at elevated temperatures.

2.2 Bulk-Reacting vs. Locally Reacting

Figure 2.5 shows a typical parallel-baffle silencer in 3D. Although the silencer itself is a 3D design, it can commonly be simplified to a 2D problem for modeling purposes. Figure 2.6 shows the two representative 2D models for the 3D parallel-baffle silencer. Figure 2.6(a) and 2.6(b) show the respective local and bulk reacting models. Before investing the time to develop a bulk-reacting analytical solution in this thesis, boundary element method (BEM) simulation was used to compare predictions using three different models. These include the 2D locally reacting BEM model, the 2D bulk-reacting BEM model and the full 3D BEM model. Since the BEM code used in this study is in three dimensions only, a 1-inch thickness sample is assumed in the normal direction for both 2D models.

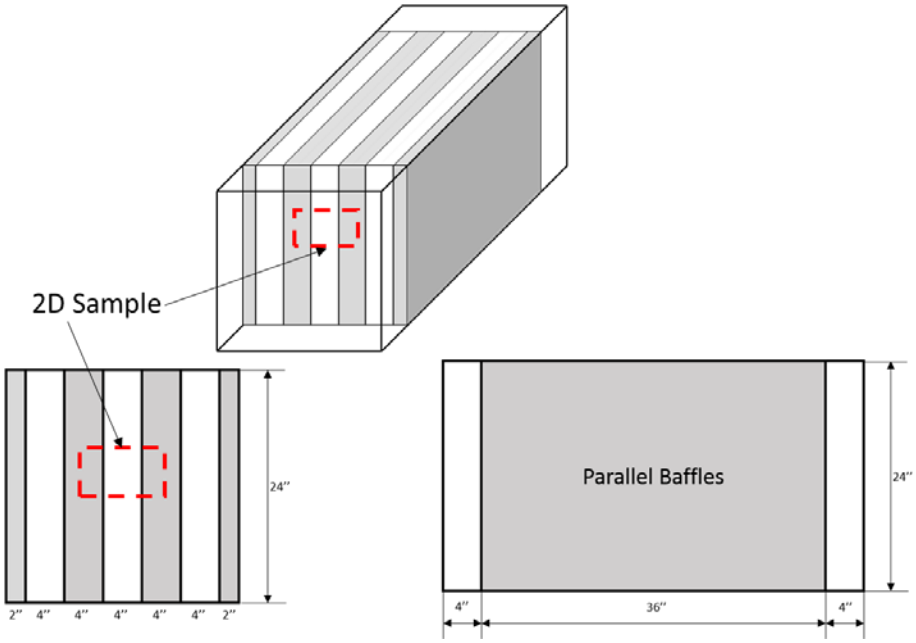

Figure 2.5: Geometry of the full parallel-baffled silencer model

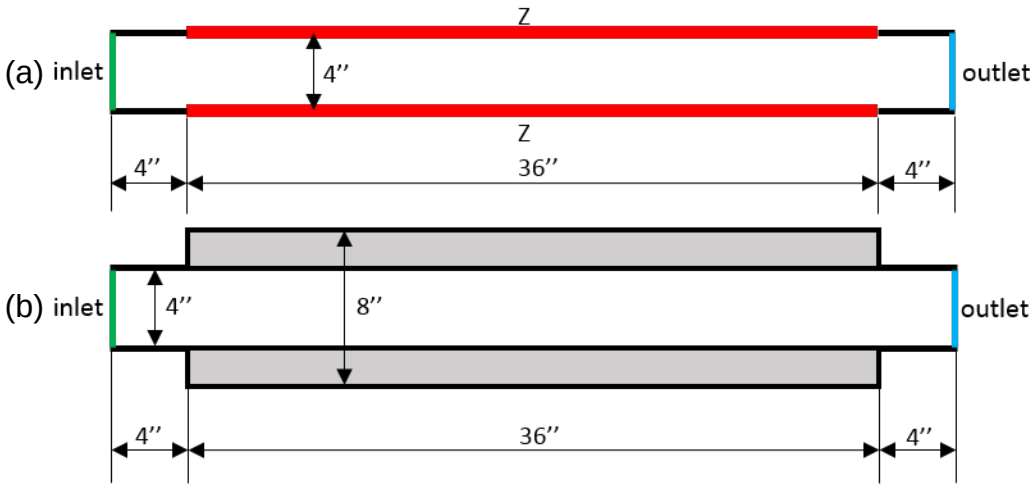

Figure 2.6: Layout of the local-reacting model (a) and the bulk-reacting model (b)

Figure 2.7 compares the BEM TL solutions of the full 3D model (Figure 2.5), 2D local impedance model (Figure 2.6(a)), and 2D bulk-reacting model (Figure 2.6 (b)). Although both 2D solutions compare fairly well with the full 3D case, the bulk-

reacting approach does provide better accuracy than the local impedance approach especially at the low frequency range.

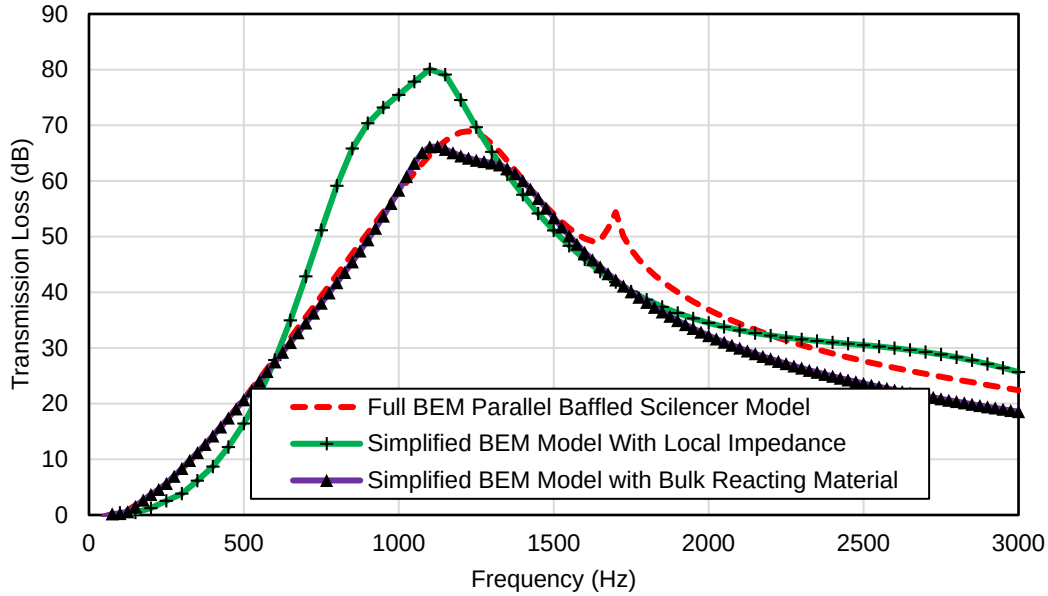

Figure 2.7: TL of 2D models vs. TL of 3D model

2.3 Perforates

2.3.1 Perforate Panels

Perforated panels are widely used between the air channel and the sound absorbing materials to protect and support the materials and improve the acoustic performance. Empirical equations for calculating transfer impedance developed over the past decades are employed as a simplified method to model the perforated panels.

Sullivan and Crocker [18] developed an empirical equation for perforated panels under room temperature and with no flow:

$$\xi = (1/\rho c\sigma)(2.4 + i0.02 f) \tag{2-23}$$

where σ is the ratio of the open area, which is also called porosity, and f is frequency in Hz. $\xi = z_{tr} / \rho c$ is the dimensionless or normalized tranfer impedance. This equation is the simplest but is still widely used.

For improved accuracy, a more detailed one was developed by Sullivan [19, 20]:

$$\xi = (1/\sigma)(0.006 + ik(t_h + 0.75 d_h)) \tag{2-24}$$

This equation takes into consideration the hole diameter d_h and the panel thickness t_h.

Coelho [21] developed an alternative expression:

$$\xi = (1/\rho c)(R_0 + iX_0) \tag{2-25}$$

where

$$R_0 = (1/\sigma)[\rho(d'/d_h)\sqrt{8\upsilon\omega} + (\rho/8c)(\omega d_h)^2] \tag{2-26}$$

and

$$X_0 = (\omega\rho/\sigma)(d'' + (d'/d_h)\sqrt{8\upsilon/\omega}) \tag{2-27}$$

with

$$d' = t_h + d_h \tag{2-28}$$

and

$$d'' = t_h + (8/3\pi)d_h(1 - 0.7\sqrt{\sigma}) \tag{2-29}$$

where υ is the kinematic viscosity of air, and $\omega = 2\pi f$.

2.3.2 Microperforate Panels (MPP)

Microperforate panel (MPP) absorbers have recently become a popular alternative to conventional perforated panels. They are lightweight and can effectively prevent fibers and other sound absorbing materials from being blown away by strong airflow. One potential downside is that the much smaller holes of MPP absorbers are more easily plugged by solid particles or grease mixed in the exhaust gas is the case for conventional perforates. If the exhaust gas is relatively clean, such as that generated from gas turbines or downstream of a perforate, the MPP may substantially improve the lifetime of silencers. The MPP can also be used to avoid the harmful effects of fibrous materials, especially in heating, ventilation, and air-conditioning (HVAC) systems.

Similar to the modeling of the conventional perforated panels, empirical equations have also been developed to model MPP. Based on Maa's work [22], Allam and Åbom in 2013 [23] have developed equations for MPP absorbers which include flow and nonlinear effects.

For MPP absorber with circular holes:

$$\xi = \frac{i\omega t_h}{\sigma c}\left(1-\frac{2}{\kappa\sqrt{-i}}\frac{J_1\left(\kappa\sqrt{-i}\right)}{J_0\left(\kappa\sqrt{-i}\right)}\right)^{-1}+\frac{2\alpha R_s}{\sigma\rho c}+\frac{|\hat{u}_h|}{\sigma c}+\frac{i\delta_c\omega\left(1+\frac{|\hat{u}_h|}{\sigma c}\right)^{-1}}{\sigma c} \qquad (2\text{-}30)$$

where $\kappa = d_h\sqrt{\omega/4\upsilon}$ is the dimensionless shear wavenumber, $\delta_c = 0.85d_h$ is the end correction term, $|\hat{u}_h|$ is the absolute value or the peak particle velocity inside the holes, $R_s = \frac{1}{2}\sqrt{2\eta\rho\omega}$ is the surface resistance, υ is kinematic viscosity, and η is the dynamic viscosity.

For MPP absorber with slit-shaped holes:

$$\xi = \frac{i\omega t_h}{\sigma c}\left(1-\frac{\tanh(\kappa\sqrt{i})}{\kappa\sqrt{i}}\right)^{-1}+\frac{2\alpha R_s}{\sigma\rho c}+\frac{|\hat{u}_h|}{\sigma c}+\frac{i\delta_s\omega\left(1+\frac{|\hat{u}_h|}{\sigma c}\right)^{-1}}{\sigma c} \qquad (2\text{-}31)$$

where $\delta_s = 0.85d_h$ is the end correction term computed by an equivalent diameter $d_h = 2\sqrt{A/\pi}$, and A is the hole area.

CHAPTER 3 FIRST-MODE ANALYTICAL SOLUTIONS FOR LINED DUCTS

In this chapter, first-mode analytical solutions are derived for rectangular and circular lined ducts. The lining in the rectangular ducts can be on one side, two sides, or four sides. The one-side case is just a special case of the two-side case if the two linings are symmetric with respect to the centerline. Both the one-side and two-side solutions are two dimensional, while the four-side solution is three-dimensional. As described in Chapter 2, the 2D solution for the rectangular lined ducts is actually a simplified solution for the full 3D parallel-baffle silencers. In all cases, both the locally reacting and the bulk-reacting solutions are presented, although the focus of this thesis is on the bulk-reacting solutions.

3.1 Rectangular Duct Lined on One Side

The simplest lined duct is the one-side lined duct. The liner is placed on one side of the duct only. The general schematic is shown in Figure 3.1. Let t denote the thickness of absorbing material, h denote the height of air channel, and b denote the width of the duct. Let $x-y$ plane denote the cross section and z denote the axial direction. Between the air channel and the absorbent material part, perforate panels are usually used to support the absorbent materials and they can improve the overall acoustic performance. Since the problem is two-dimensional in the $y-z$ plane by nature and b can be assumed very small, there is no variation in the x direction.

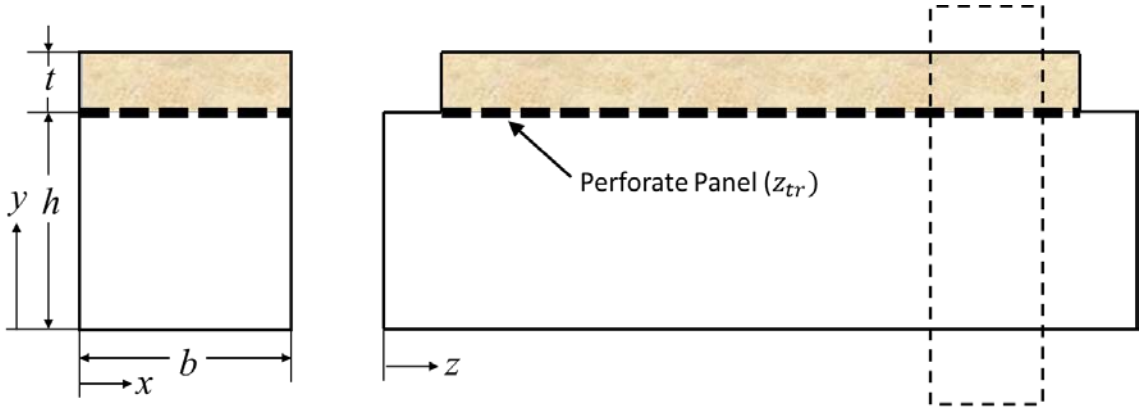

Figure 3.1 Schematic of 1-side Lined Duct

3.1.1 Locally Reacting Method

In the locally reacting method, the straight-duct four-pole transfer matrix $[T]$ is employed in the y direction of the air channel, which means sound pressure distribution in the y direction is not uniform and the wavenumber k can be decomposed into the y and z directions. The boundary condition at $y = h$ is described by a uniform local impedance Z that does not change along the z direction. The value of Z is the sum of the local impedance of the liner material itself and the transfer impedance z_{tr} of the perforated panel.

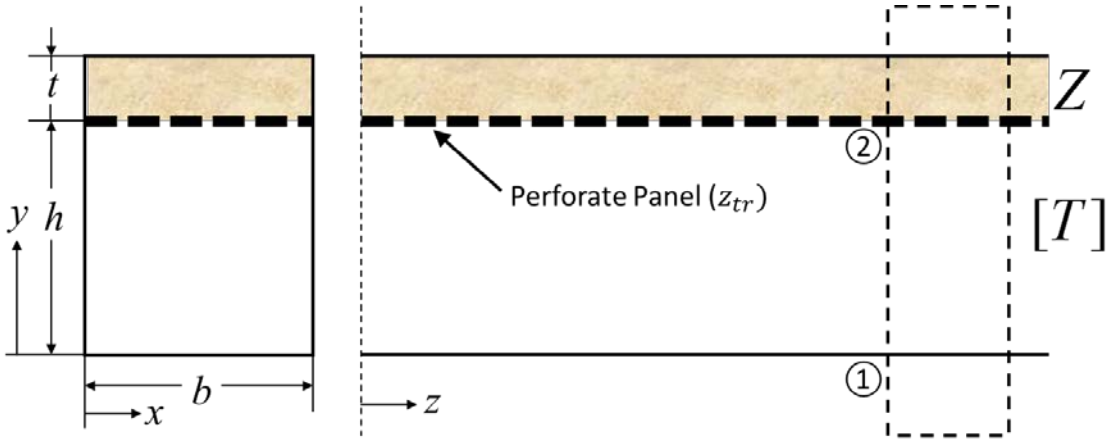

Figure 3.2 Schematic of 1-side Locally Recating Model

Therefore, from position 1 ($y = 0$) to position 2 ($y = h$), the four-pole transfer matrix is

$$[T] = \begin{bmatrix} \cos(k_y h) & \frac{i\rho\omega}{k_y}\sin(k_y h) \\ \frac{ik_y}{\rho\omega}\sin(k_y h) & \cos(k_y h) \end{bmatrix} \tag{3-1}$$

where k_y is the $y-$component of the wavenumber, ρ is the density, $\omega = 2\pi f$ is the circular frequency, and $i = \sqrt{-1}$.

Applying the rigid-wall boundary condition at position 1 and the local impedance boundary condition at position 2:

$$\begin{cases} u_1 = 0 \\ \frac{p_2}{u_2} = Z + z_{tr} \end{cases} \tag{3-2}$$

the characteristic equation can be obtained:

$$i(Z + z_{tr})k_y \tan(k_y h) + \rho\omega = 0 \tag{3-3}$$

In some literature, the normalized admittance $\eta = \frac{\rho c}{Z}$ is used and the characteristic equation can be rewritten as:

$$(1 + \xi\eta)\ k_y \tan(k_y h) - ik\eta = 0 \tag{3-4}$$

The above equation can be solved for k_y by using a nonlinear equation solver. According to Ingard [7], the initial guess to the nonlinear characteristic equation can be obtained by solving an approximate equation which ignores the transfer impedance of the perforated panel. The low frequency approximation is

$$(k_y h)^2 \approx -ikh\eta \tag{3-5}$$

The high frequency approximation is

$$k_y h \approx \frac{\pi}{2} \tag{3-6}$$

With the relationship,

$$k_y^2 + k_z^2 = k^2 \tag{3-7}$$

k_z can be obtained afterwards. Sound attenuation in dB at a distance z can be found from

$$20\log_{10}\frac{|\,p(0)\,|}{|\,p(z)\,|} = -20\log_{10}(e)k_{zi}z \approx -8.72k_{zi}z \qquad (3\text{-}8)$$

where $p(0)$ and $p(z)$ are sound pressure at the inlet and at distance z, respectively, and k_{zi} is the imaginary part of k_z.

3.1.2 Bulk-Reacting Method

The four-pole transfer matrix is employed in the y direction for each component in the bulk-reacting method. The method is applied to the 2D case with the absorbent liner on one side. The 2D bulk-reacting method models the silencer in the y and z directions. Figure 3.3 shows a schematic of the bulk-reacting model.

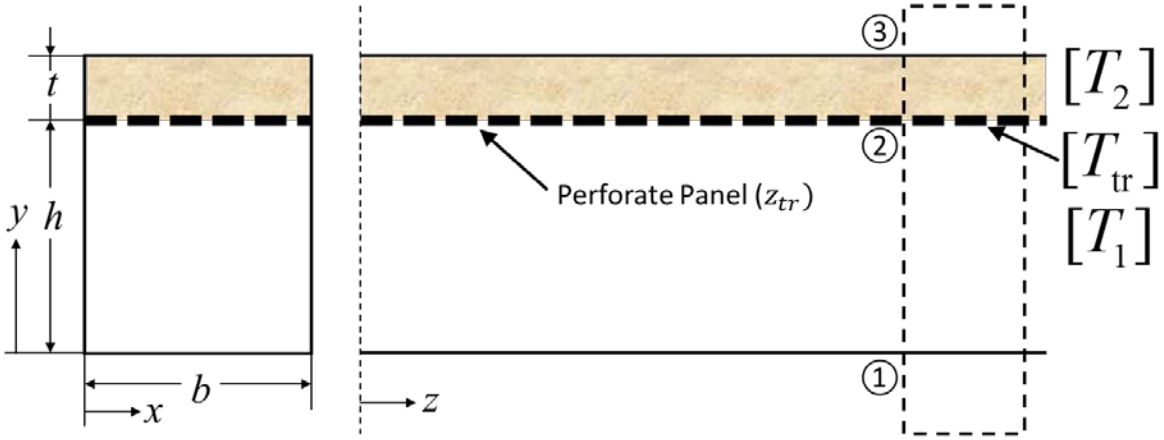

Figure 3.3 Schematic of the One-Side Bulk-Recating Model

The transfer matrix $[T_1]$ and $[T_2]$ are used to model the air channel and the absorber , respectively, in the y direction. $[T_1]$ and $[T_2]$ can be expressed as

$$[T_1]=\begin{bmatrix} \cos(k_y h) & \frac{i\rho\omega}{k_y}\sin(k_y h) \\ \frac{ik_y}{\rho\omega}\sin(k_y h) & \cos(k_y h) \end{bmatrix} \tag{3-9}$$

$$[T_2]=\begin{bmatrix} \cos(k_y^* t) & \frac{i\rho^*\omega}{k_y^*}\sin(k_y^* t) \\ \frac{ik_y^*}{\rho^*\omega}\sin(k_y^* t) & \cos(k_y^* t) \end{bmatrix} \tag{3-10}$$

where k_y^* is the $y-$direction wavenumber in the absorber, d is the thickness of the absorber, ρ^* is the complex density of the absorber, ρ is the density of air, D is the width of the air channel, k_y is the $y-$direction wavenumber in air, $\omega = 2\pi f$ is the circular frequency, and $i=\sqrt{-1}$.

The behavior of the perforate panel between the air channel and the absorber is presented by a transfer impedance matrix $[T_{tr}]$:

$$[T_{tr}]=\begin{bmatrix} 1 & z_{tr} \\ 0 & 1 \end{bmatrix} \tag{3-11}$$

Multiply the above three matrices together to obtain the resultant transfer matrix $[T]$ relating position 1 to position 3:

$$\begin{Bmatrix} p_1 \\ u_1 \end{Bmatrix} = [T] \begin{Bmatrix} p_3 \\ u_3 \end{Bmatrix} = \begin{bmatrix} t_{11} & t_{12} \\ t_{21} & t_{22} \end{bmatrix} \begin{Bmatrix} p_3 \\ u_3 \end{Bmatrix} \tag{3-12}$$

where $[T] = [T_1][T_{tr}][T_2]$, p_1 and u_1 are the sound pressure and particle velocity at position 1, and p_3 and u_3 are the sound pressure and particle velocity at position 3.

Apply the rigid-wall boundary condition at positions 1 and 3:

$$u_1 = u_3 = 0 \tag{3-13}$$

Then, the characteristic equation can be found by setting t_{21} to be zero. In other words,

$$\rho k_y^* \tan(k_y^* t) + i k_y k_y^* z_{tr} \tan(k_y h) \tan(k_y^* t) / \omega + \rho^* k_y \tan(k_y h) = 0 \tag{3-14}$$

$$k_y^2 + k_z^2 = k^2 \tag{3-15}$$

$$k_y^{*2} + k_z^{*2} = k^{*2} \tag{3-16}$$

and the continuity of the wavenumber in the $z-$direction (Selamet et al. [24]):

$$k_z^* = k_z \tag{3-17}$$

k_y becomes the only unknown and can be solved by a nonlinear equation solver. The low frequency and high frequency approximations are the same as the locally reacting method. And sound attenuation in dB at a distance z is

$$20\log_{10}\frac{|p(0)|}{|p(z)|} = -20\log_{10}(e)k_{zi}z \approx -8.72k_{zi}z \qquad (3\text{-}18)$$

where $p(0)$ and $p(z)$ are sound pressure at the inlet and at distance z respectively, and k_{zi} is the imaginary part of k_z.

3.2 Rectangular Duct Lined on Two Sides

3.2.1 Locally Reacting Method

The layout of the problem is shown in Figure 3.4. Also, the four-pole transfer matrix is only employed in the air channel.

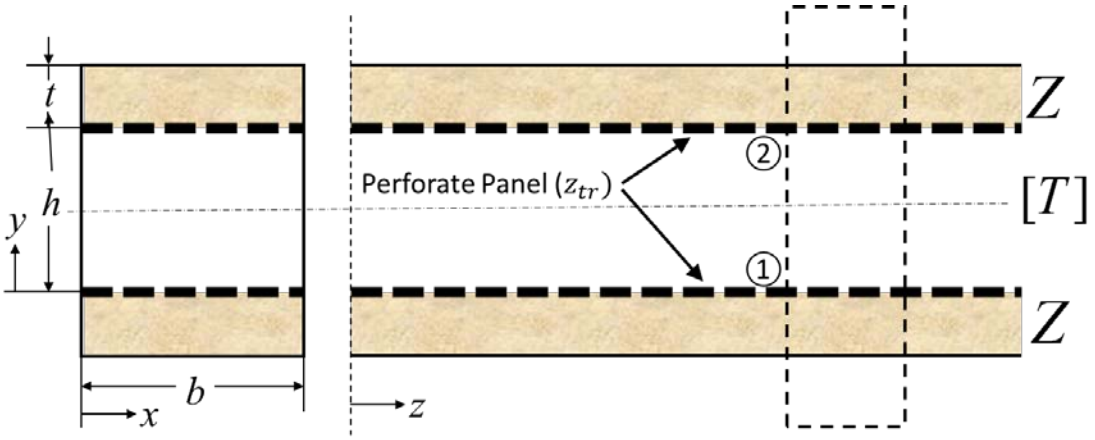

Figure 3.4 Schematic of 2-side Locally Recating Model

From position 1 ($y = 0$) to position 2 ($y = h$), the four-pole transfer matrix is

$$[T]=\begin{bmatrix} \cos(k_y h) & \dfrac{i\rho\omega}{k_y}\sin(k_y h) \\ \dfrac{ik_y}{\rho\omega}\sin(k_y h) & \cos(k_y h) \end{bmatrix} \tag{3-19}$$

Apply the boundary conditions at position 1 and position 2:

$$\frac{p_1}{-u_1}=\frac{p_2}{u_2}=Z+z_{tr} \tag{3-20}$$

and the following characteristic equation can be obtained:

$$\frac{k_y}{k}\tan(k_y h)+\tan(k_y h)\frac{k}{k_y}\frac{\eta^2}{(1+\xi\eta)^2}-\frac{2i\eta}{1+\xi\eta}=0 \tag{3-21}$$

According to Ingard [7], the initial guess to the nonlinear characteristic equation can be obtained by solving an approximate equation which ignores the transfer impedance of the perforated panel. The low frequency approximation is

$$\left(\frac{k_y}{k}\right)^2 \approx \frac{-2i\eta}{kh} \tag{3-22}$$

The high frequency approximation is

$$k_y h \approx \pi-\frac{2i\pi}{\eta kh} \tag{3-23}$$

Afterwards, sound attenuation in dB at a distance z can be obtained as usual.

3.2.2 Bulk-Reacting Method

The four-pole transfer matrix is employed for each component in the bulk-reacting method. Figure 3.5 shows a schematic of the two-side lining model.

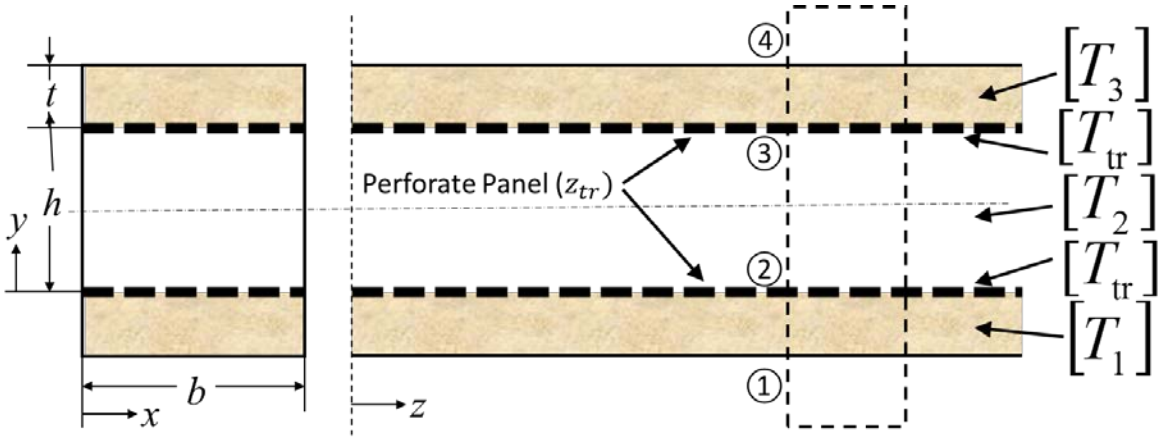

Figure 3.5 Schematic of the Two-Side Bulk-Recating Model

The transfer matrices $[T_1]$, $[T_2]$ and $[T_3]$, are used to model the absorber parts and air channel in the y direction. $[T_1]$, $[T_2]$ and $[T_3]$ can be expressed as

$$[T_1]=[T_3]=\begin{bmatrix} \cos(k_y^* t) & \frac{i\rho^*\omega}{k_y^*}\sin(k_y^* t) \\ \frac{ik_y^*}{\rho^*\omega}\sin(k_y^* t) & \cos(k_y^* t) \end{bmatrix} \tag{3-24}$$

$$[T_2]=\begin{bmatrix} \cos(k_y h) & \frac{i\rho\omega}{k_y}\sin(k_y h) \\ \frac{ik_y}{\rho\omega}\sin(k_y h) & \cos(k_y h) \end{bmatrix} \tag{3-25}$$

The behavior of the perforated panel between the air channel and the absorber is represented by a transfer impedance matrix $[T_{tr}]$:

$$[T_{tr}] = \begin{bmatrix} 1 & z_{tr} \\ 0 & 1 \end{bmatrix} \tag{3-26}$$

where z_{tr} is the transfer impedance of the perforated panel.

Multiply the five matrices together to obtain the resultant transfer matrix $[T]$ relating position 1 to position 4:

$$\begin{Bmatrix} p_1 \\ u_1 \end{Bmatrix} = [T] \begin{Bmatrix} p_4 \\ u_4 \end{Bmatrix} = \begin{bmatrix} t_{11} & t_{12} \\ t_{21} & t_{22} \end{bmatrix} \begin{Bmatrix} p_4 \\ u_4 \end{Bmatrix} \tag{3-27}$$

where $[T] = [T_1][T_{tr}][T_2][T_{tr}][T_3]$, p_1 and u_1 are the sound pressure and particle velocity at position 1, and p_4 and u_4 are the sound pressure and particle velocity at position 4, respectively.

Apply the rigid-wall boundary condition at positions 1 and 4

$$u_1 = u_4 = 0 \tag{3-28}$$

and the continuity of the wavenumber in the $z-$direction (Selamet et al. [24]),

$$k_z^* = k_z \tag{3-29}$$

Afterwards, the characteristic equation can be obtained by setting t_{21} to be zero. The low frequency and high frequency approximations are the same as the locally reacting method. After solving the nonlinear characteristic equation for k_y, k_z can be found from

$$k_z = \sqrt{k^2 - k_y^2} \tag{3-30}$$

and sound attenuation in dB at a distance z can been obtained as usual.

3.3 Rectangular Duct Lined on Four Sides

The more complicated problem is the four-side lined duct problem. The schematic of a typical four-side 3D rectangular lined duct is shown in Figure 3.6. The 3D rectangular lined duct can be modeled by a combination of two 2D lined ducts in the x and y directions, respectively.

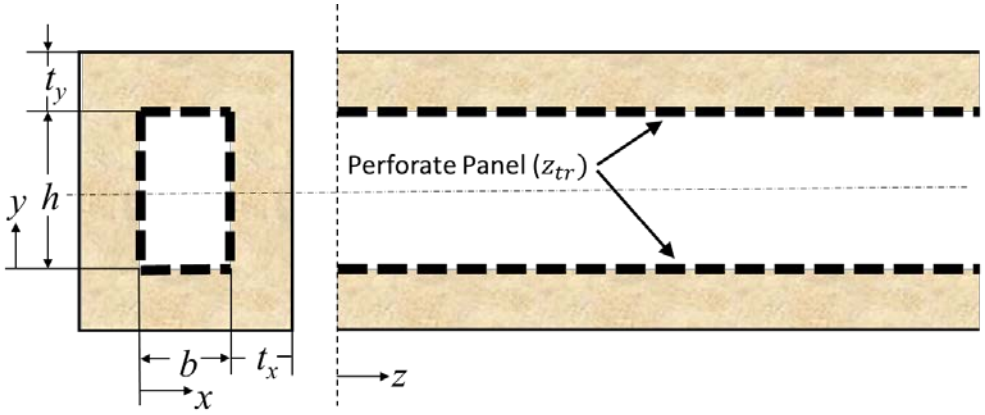

Figure 3.6 Schematic of 4-side Lining Lined Duct

3.3.1 Locally Reacting Method

The layout of the 3D locally reacting problem is shown in Figure 3.7. The four-pole transfer matrix is applied in the air channel in x and y directions, respectively.

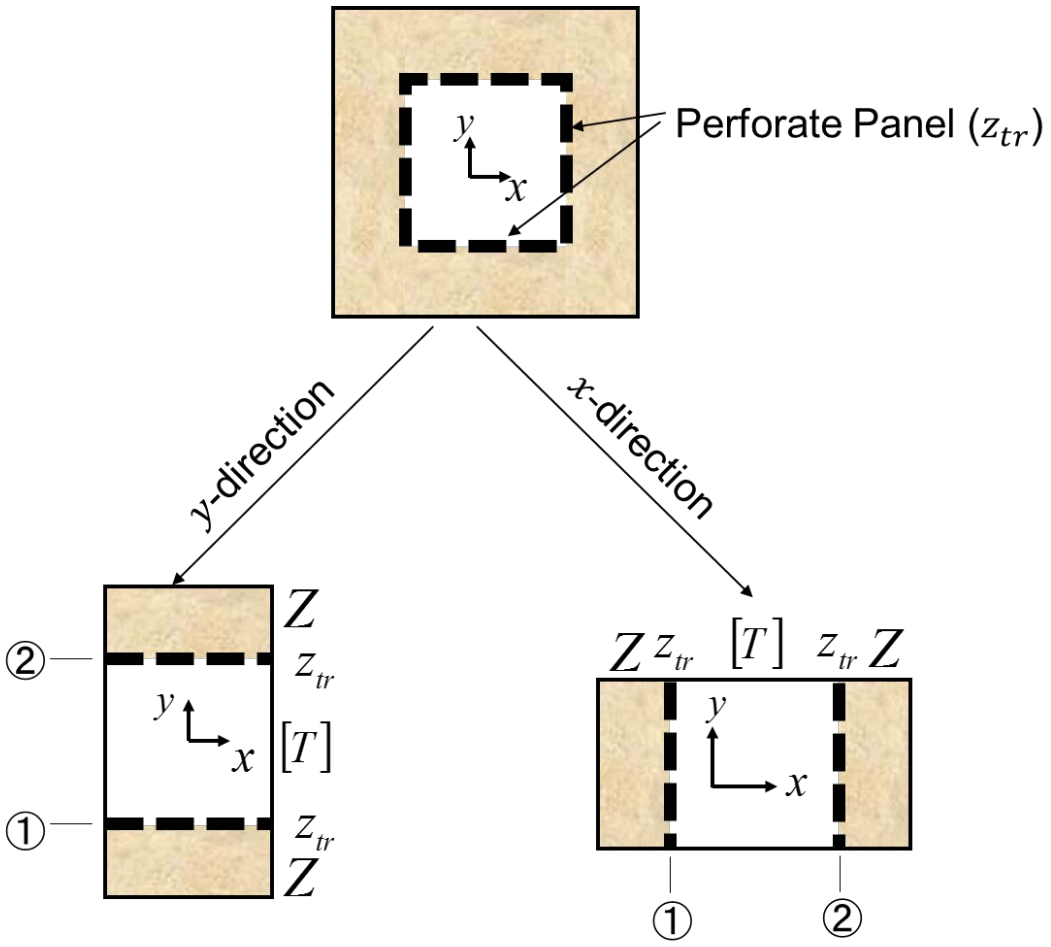

Figure 3.7 Schematic of 4-side Locally Recating Model

In the y direction, from position 1 to position 2, the four-pole transfer matrix is

$$[T]=\begin{bmatrix} \cos(k_y h) & \frac{i\rho\omega}{k_y}\sin(k_y h) \\ \frac{ik_y}{\rho\omega}\sin(k_y h) & \cos(k_y h) \end{bmatrix} \tag{3-31}$$

Apply the boundary conditions at position 1 and position 2:

$$\frac{p_1}{-u_1}=\frac{p_2}{u_2}=Z+z_{tr} \tag{3-32}$$

Then, the following characteristic equation can be obtained:

$$\frac{k_y}{k}\tan(k_y h)+\tan(k_y h)\frac{k}{k_y}\frac{\eta^2}{(1+\xi\eta)^2}-\frac{2i\eta}{1+\xi\eta}=0 \tag{3-33}$$

where η is the normalized admittance defined previously:

$$\eta=\frac{i\rho c\tan(k^* t_y)}{\rho^* c^*} \tag{3-34}$$

k_y can be solved from the characteristic equation using a nonlinear equation solver.

Perform the same procedure in the x direction. From position 1 to position 2, the four-pole transfer matrix is

$$[T]=\begin{bmatrix} \cos(k_y b) & \frac{i\rho\omega}{k_y}\sin(k_y b) \\ \frac{ik_y}{\rho\omega}\sin(k_y b) & \cos(k_y b) \end{bmatrix} \tag{3-35}$$

Apply the boundary conditions at position 1 and position 2:

$$\frac{p_1}{-u_1}=\frac{p_2}{u_2}=Z+z_{tr} \tag{3-36}$$

and the characteristic equation can be obtained:

$$\frac{k_x}{k}\tan(k_x b)+\tan(k_x b)\frac{k}{k_x}\frac{\eta^2}{(1+\xi\eta)^2}-\frac{2i\eta}{1+\xi\eta}=0 \tag{3-37}$$

Therefore, a set of two independent characteristic equations can be obtained. Solve the two equations separately for k_y and k_x using a nonlinear solver, and k_z can be calculated from the following equation:

$$k^2-k_x^2-k_y^2=k_z^2 \tag{3-38}$$

Sound attenuation in dB at a distance z can be found by using

$$20\log_{10}\frac{|p(0)|}{|p(z)|}=-20\log_{10}(e)k_{zi}z\approx-8.72k_{zi}z \tag{3-39}$$

where $p(0)$ and $p(z)$ are sound pressure at the inlet and at distance z, respectively, and k_{zi} is the imaginary part of k_z.

3.3.2 Bulk-Reacting Method

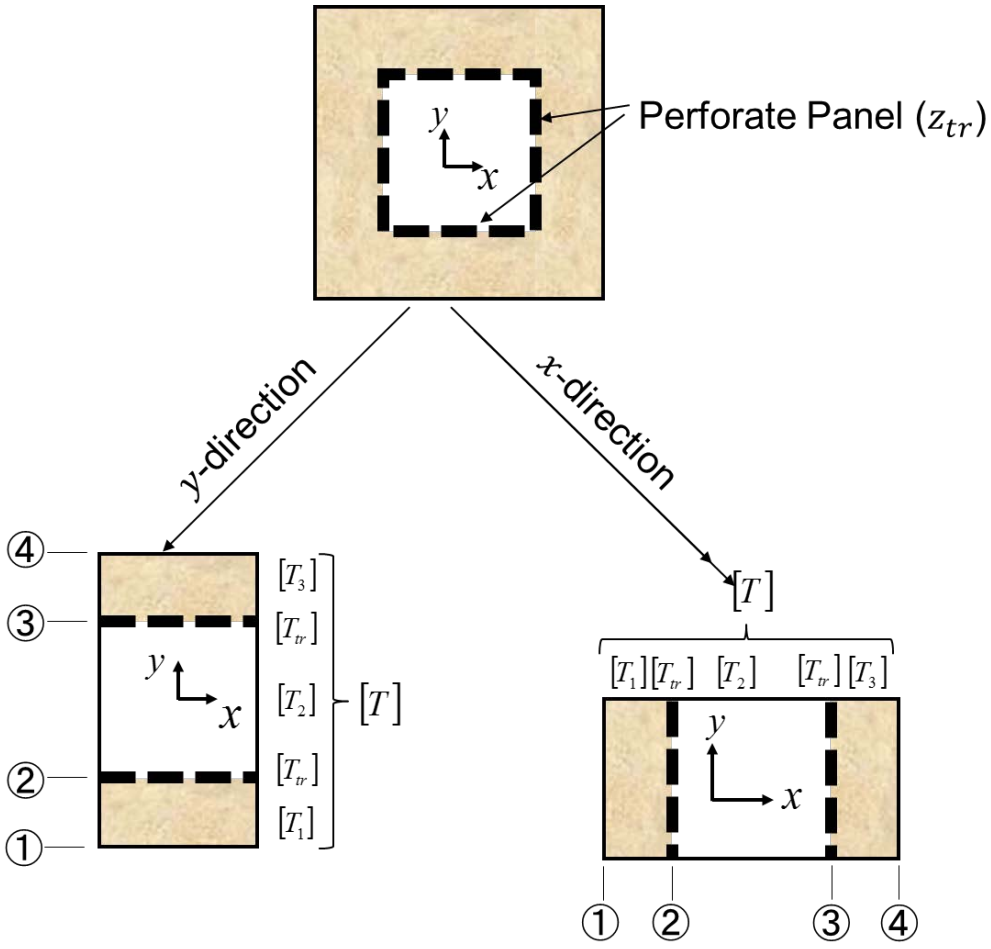

Figure 3.8 Schematic of 4-side Bulk-Recating Model

The layout of the 3D four-side bulk-reacting problem is shown in Figure 3.8. In the y direction, the transfer matrices $[T_1]$, $[T_2]$ and $[T_3]$, are used to model the absorber parts and the air channel. $[T_1]$, $[T_2]$ and $[T_3]$ can be expressed as

$$[T_1]=[T_3]=\begin{bmatrix} \cos(k_y^* t) & \dfrac{i\rho^*\omega}{k_y^*}\sin(k_y^* t) \\ \dfrac{ik_y^*}{\rho^*\omega}\sin(k_y^* t) & \cos(k_y^* t) \end{bmatrix} \tag{3-40}$$

$$[T_2]=\begin{bmatrix} \cos(k_y h) & \dfrac{i\rho\omega}{k_y}\sin(k_y h) \\ \dfrac{ik_y}{\rho\omega}\sin(k_y h) & \cos(k_y h) \end{bmatrix} \tag{3-41}$$

The behavior of the perforated panel between the air channel and the absorber is represented by a transfer impedance matrix $[T_{tr}]$:

$$[T_{tr}]=\begin{bmatrix} 1 & z_{tr} \\ 0 & 1 \end{bmatrix} \tag{3-42}$$

where z_{tr} is the transfer impedance of the perforated panel positioned between the air channel and the absorber.

Multiplying the five matrices together, a resultant transfer matrix $[T]$ is generated to relate position 1 to position 4:

$$\begin{Bmatrix} p_1 \\ u_1 \end{Bmatrix} = [T] \begin{Bmatrix} p_4 \\ u_4 \end{Bmatrix} = \begin{bmatrix} t_{11} & t_{12} \\ t_{21} & t_{22} \end{bmatrix} \begin{Bmatrix} p_4 \\ u_4 \end{Bmatrix} \tag{3-43}$$

where $[T] = [T_1][T_{tr}][T_2][T_{tr}][T_3]$, p_1 and u_1 are the sound pressure and particle velocity at position 1, respectively, and p_4 and u_4 are the sound pressure and particle velocity at position 4, respectively.

The decomposition of wavenumber in the air channel is:

$$k_x^2 + k_y^2 + k_z^2 = k^2 \tag{3-44}$$

Similarly, the decomposition of the wavenumber in the absorbing material is:

$$k_x^{*2} + k_y^{*2} + k_z^{*2} = k^{*2} \tag{3-45}$$

For the absorbing material layer at the top and the bottom, if we remove the four corners and apply the rigid-wall boundary condition, the first-mode solution requires.

$$k_x^* = \frac{\pi}{b} \tag{3-46}$$

The wavenumber in the z direction is the same for both the absorbing material and air. In other words,

$$k_z = k_z^* \tag{3-47}$$

Therefore,

$$k_y^* = \sqrt{k^{*^2} - k^2 + k_x^2 + k_y^2 - (\frac{\pi}{b})^2} \tag{3-48}$$

In the y direction, the transfer matrices $[T_1]$, $[T_2]$ and $[T_3]$, are used to model the absorber parts and the air channel. $[T_1]$, $[T_2]$ and $[T_3]$ can be expressed as

$$[T_1] = [T_3] = \begin{bmatrix} \cos(k_x^* t) & \frac{i\rho^* \omega}{k_x^*} \sin(k_x^* t) \\ \frac{ik_x^*}{\rho^* \omega} \sin(k_x^* t) & \cos(k_x^* t) \end{bmatrix} \tag{3-49}$$

$$[T_2] = \begin{bmatrix} \cos(k_x h) & \frac{i\rho\omega}{k_x} \sin(k_x h) \\ \frac{ik_x}{\rho\omega} \sin(k_x h) & \cos(k_x h) \end{bmatrix} \tag{3-50}$$

The behavior of the perforated panel between the air channel and the absorber is simulated by the by a transfer impedance matrix $[T_{tr}]$:

$$[T_{tr}] = \begin{bmatrix} 1 & z_{tr} \\ 0 & 1 \end{bmatrix} \tag{3-51}$$

Multiplying the five matrices together, a resultant transfer matrix $[T]$ is generated to relate position 1 to position 4 in the x direction.

$$\begin{Bmatrix} p_1 \\ u_1 \end{Bmatrix} = [T] \begin{Bmatrix} p_4 \\ u_4 \end{Bmatrix} = \begin{bmatrix} t_{11} & t_{12} \\ t_{21} & t_{22} \end{bmatrix} \begin{Bmatrix} p_4 \\ u_4 \end{Bmatrix} \tag{3-52}$$

The decomposition of wavenumber in the air channel is:

$$k_x^2 + k_y^2 + k_z^2 = k^2 \tag{3-53}$$

Similarly, the decomposition of the wavenumber in the absorbing material is:

$$k_x^{*^2} + k_y^{*^2} + k_z^{*^2} = k^{*^2} \tag{3-54}$$

For the absorbing material layer at the left side and the right side, if we remove the four corners and apply the rigid-wall boundary condition, the first-mode solution requires

$$k_y^* = \frac{\pi}{h} \tag{3-55}$$

The wavenumber in the z direction is the same for both the absorbing material and air. In other words,

$$k_z = k_z^* \tag{3-56}$$

Therefore,

$$k_x^* = \sqrt{k^{*^2} - k^2 + k_x^2 + k_y^2 - (\frac{\pi}{h})^2} \tag{3-57}$$

The rigid-wall boundary conditions require t_{21} of the resultant $[T]$ in the y direction and t_{21} of the resultant $[T]$ in the x direction to be zero at the same time. Therefore,

a set of two characteristic equations can be obtained. Solve the two equations simultaneously for k_x and k_y. After that, k_z can be calculated from Equation (3-49).

Sound attenuation in dB at a distance z can be found by using

$$20\log_{10}\frac{|p(0)|}{|p(z)|} = -20\log_{10}(e)k_{zi}z \approx -8.72k_{zi}z \tag{3-58}$$

where $p(0)$ and $p(z)$ are the sound pressure values at the inlet and at a distance z, respectively, and k_{zi} is the imaginary part of k_z.

3.4 Circular Lined Ducts

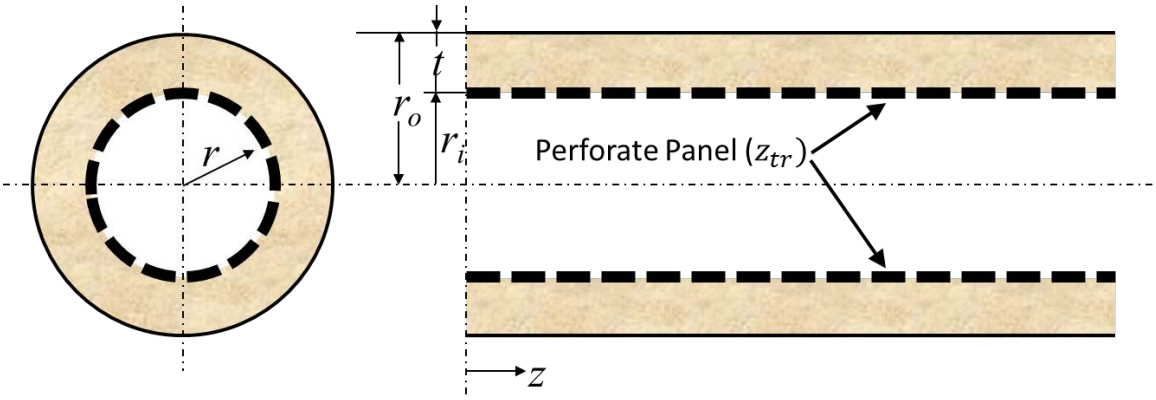

Figure 3.9 Schematic of Circular Lined Duct

The schematic of a typical circular lined duct is shown in Figure 3.9. Let r_i denote the air channel radius, r_o denote the outer radius of the liner, and t denote the thickness of the sound absorbing liner.

3.4.1 Locally Reacting Method

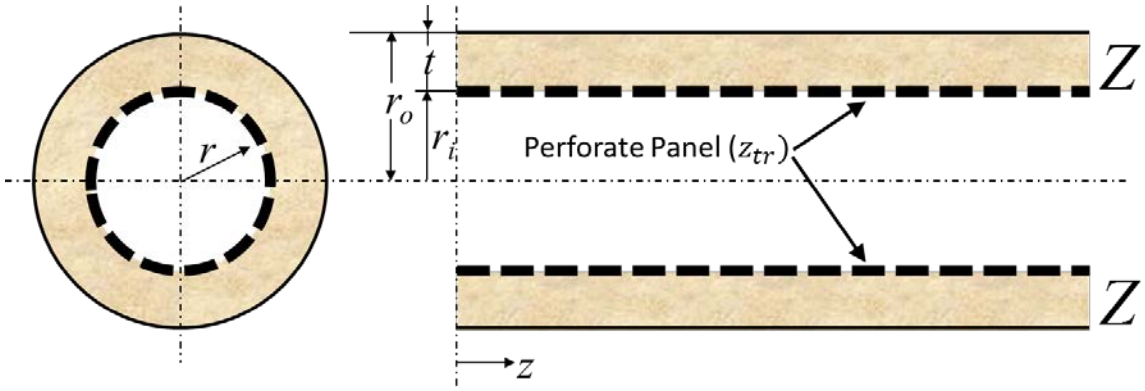

Figure 3.10 Locally Recating Model of Circular Lined Duct

The sound pressure in the air channel part in the radial direction can be expressed as:

$$p = AJ_0(k_r r) \tag{3-59}$$

and the corresponding particle velocity is:

$$u = \frac{-iAk_r}{\rho\omega} J_1(k_r r) \tag{3-60}$$

where J_0 is the 0th-order Bessel function of the 1st kind, J_1 is the 1st-order Bessel function of the 1st kind, k_r is the wavenumber of air in the radial direction, and r is the radial coordinate of the field point.

The following boundary condition represents the dimensionless normal admittance at $r = r_i$

$$\eta = -i(\frac{k_r}{k})(\frac{J_1(k_r r_i)}{J_0(k_r r_i)}) \tag{3-61}$$

where according to Ingard [7]

$$\eta = \frac{\rho c(J_1(k_r^* r_i)Y_1(k_r^* r_o) - J_1(k_r^* r_o)Y_1(k_r^* r_i))}{i\rho^* c^*(J_0(k_r^* r_i)Y_1(k_r^* r_o) - J_1(k_r^* r_o)Y_0(k_r^* r_i))} \tag{3-62}$$

According to Ingard [7], the initial guess to the nonlinear characteristic equation can be obtained by solving an approximate equation which ignores the transfer impedance of the perforated panel. The low frequency approximation is

$$(k_r r_i)^2 \approx -i2kr_i\eta \tag{3-63}$$

The high frequency approximation is

$$k_r r_i \approx \frac{3\pi}{4}\left(1 - \frac{i}{kr_i\eta}\right) \tag{3-64}$$

Therefore, k_r can be obtained from the characteristic equation (3-61). Afterwards, k_z can be obtained from

$$k_r^2 + k_z^2 = k^2 \tag{3-65}$$

Sound attenuation in dB at a distance z can be found by using

$$20\log_{10}\frac{|p(0)|}{|p(z)|} = -20\log_{10}(e)k_{zi}z \approx -8.72k_{zi}z \tag{3-66}$$

where $p(0)$ and $p(z)$ are the sound pressure at the inlet and at a distance z, respectively, and k_{zi} is the imaginary part of k_z.

3.4.2 Bulk-Reacting Method

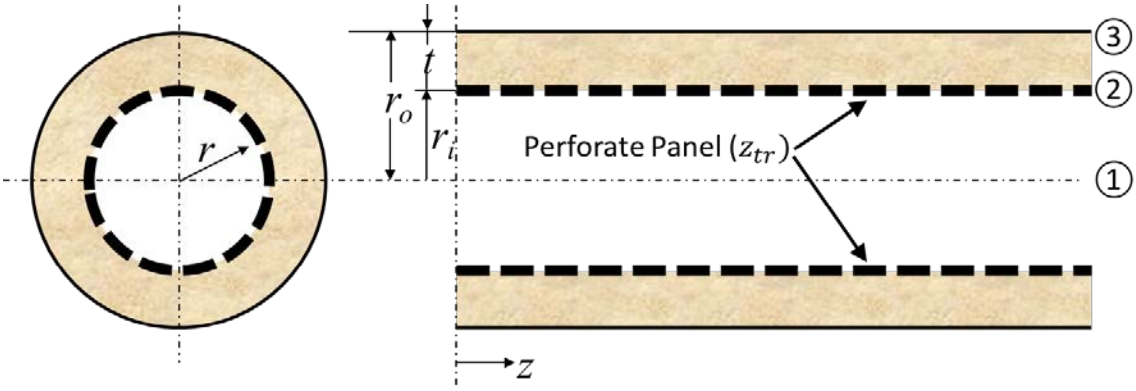

Figure 3.11 Bulk-Recating Model of Circular Lined Duct

As shown in Figure 3.11, position 1 refers to the central axis of the air channel, position 2 refers to the perforated panel between the air channel and the sound absorbing layer, and position 3 refers to the exterior boundary of the circular duct. Sound pressure in the air channel in the radial direction can be expressed as

$$p = AJ_0(k_r r) \tag{3-67}$$

The corresponding particle velocity is

$$u = \frac{i}{\rho\omega}\frac{dp}{dr} = \frac{i}{\rho\omega}Ak_r(-J_1(k_r r)) \tag{3-68}$$

Sound pressure in the sound absorbing material is

$$p^* = BJ_0(k_r^* r) + CY_0(k_r^* r) \tag{3-69}$$

The corresponding particle velocity is

$$u^* = \frac{i}{\rho^* \omega}\frac{dp^*}{dr} = \frac{iBk_r^*}{\rho^* \omega}(-J_1(k_r^* r)) + \frac{iCk_r^*}{\rho^* \omega}(-Y_1(k_r^* r)) \tag{3-70}$$

where k_r^* is the wavenumber in the absorber in the radial direction, Y_1 is the 1st-order Bessel function of the 2nd kind. The following boundary conditions are then applied:

$$\begin{cases} p_2 - p_2^* = z_{tr} u_2 \\ u_2 = u_2^* \\ u_3 = 0 \end{cases} \tag{3-71}$$

This results in the following matrix equation:

$$\begin{bmatrix} J_0(k_r r_i) + \dfrac{Z_{tr} k_r}{\rho\omega} J_1(k_r r_i) & -J_0(k_r^* r_i) & -Y_0(k_r^* r_i) \\ \dfrac{\rho^* k_r}{\rho k_r^*} J_1(k_r r_i) & J_1(k_r^* r_i) & Y_1(k_r^* r_i) \\ 0 & J_1(k_r^* r_o) & CY_1(k_r^* r_o) \end{bmatrix} \begin{Bmatrix} A \\ B \\ C \end{Bmatrix} = \begin{Bmatrix} 0 \\ 0 \\ 0 \end{Bmatrix} \tag{3-72}$$

By setting the determinate to zero, a characteristic equation can be obtained and k_r can be solved from the characteristic equation. The low frequency and high frequency approximations are the same as the locally reacting method. Afterwards, k_z can be obtained from

$$k_z = \sqrt{k^2 - k_r^2} \tag{3-73}$$

Sound attenuation in dB at a distance z can be found by using

$$20\log_{10}\frac{|p(0)|}{|p(z)|} = -20\log_{10}(e)k_{zi}z \approx -8.72k_{zi}z \tag{3-74}$$

where $p(0)$ and $p(z)$ are the sound pressure at the inlet and at a distance z, respectively, and k_{zi} is the imaginary part of k_z.

The methodology of the 2D bulk-reacting analytical solutions for rectangular lined ducts with lining on one side and two sides, as well as 3D bulk-reacting analytical solutions for rectangular lined ducts with sound absorbing material on four sides and circular lined ducts has been presented in this chapter. The locally reacting method has been reproduced at the same time.

CHAPTER 4 VERIFICATIONS AND DISCUSSIONS

In this chapter, the first-mode analytical solutions developed in Chapter 3 are compared to the direct mixed-body boundary element method (BEM) [4] solutions. Since the BEM used in this study is three dimensional, a one-inch thickness is assumed in the 3D BEM models when compared to the 2D analytical solutions for rectangular ducts lined on two sides. For rectangular ducts lined on all four sides and circular ducts, the analytical solutions themselves are three-dimensional already. If the cross section of a duct becomes large enough so that higher-order modes begin to emerge, a so-called “impedance-to-scattering matrix method” [5] is also applied in the BEM to calculate the TL at high frequencies.

It should be noted that the analytical solutions developed in this thesis are the first-mode solutions only while the BEM can theoretically include all higher-order modes. In addition, the analytical solutions calculate sound attenuation while the BEM calculates TL. As mentioned previously, these differences may become negligible for large dissipative silencers with a simple and uniform cross section.

4.1 Rectangular Ducts Lined on Two Sides

Both the locally reacting and bulk-reacting analytical solutions are compared to the corresponding BEM solutions. The first two test cases are the rectangular lined ducts modeled by the local impedance approach. The lining has a flow resistivity equal to 16,000 Rayls/m and test case (a) is covered by a 30% porosity perforated panel while test case (b) is covered by a 15% porosity perforated panel. The

temperature is set at room temperature. The geometry of the test case is shown in Figure 4.1.

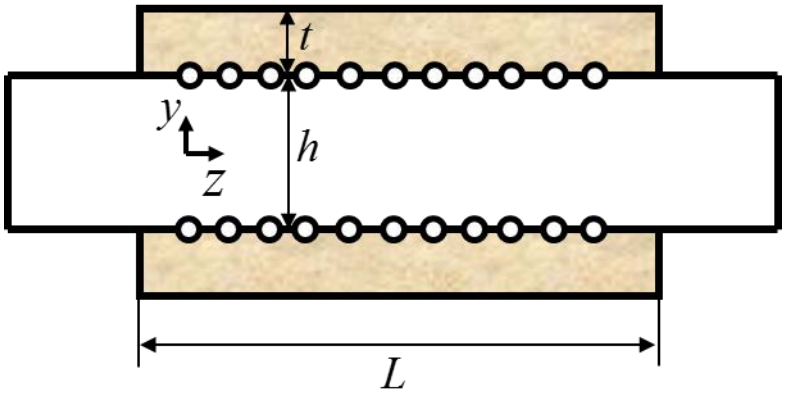

Figure 4.1 Geometry of 2D test case

Figure 4.2 compares the locally reacting analytical solutions to the corresponding BEM solutions for two different designs. In both designs, the locally reacting analytical solutions agree very well with the corresponding BEM solutions.

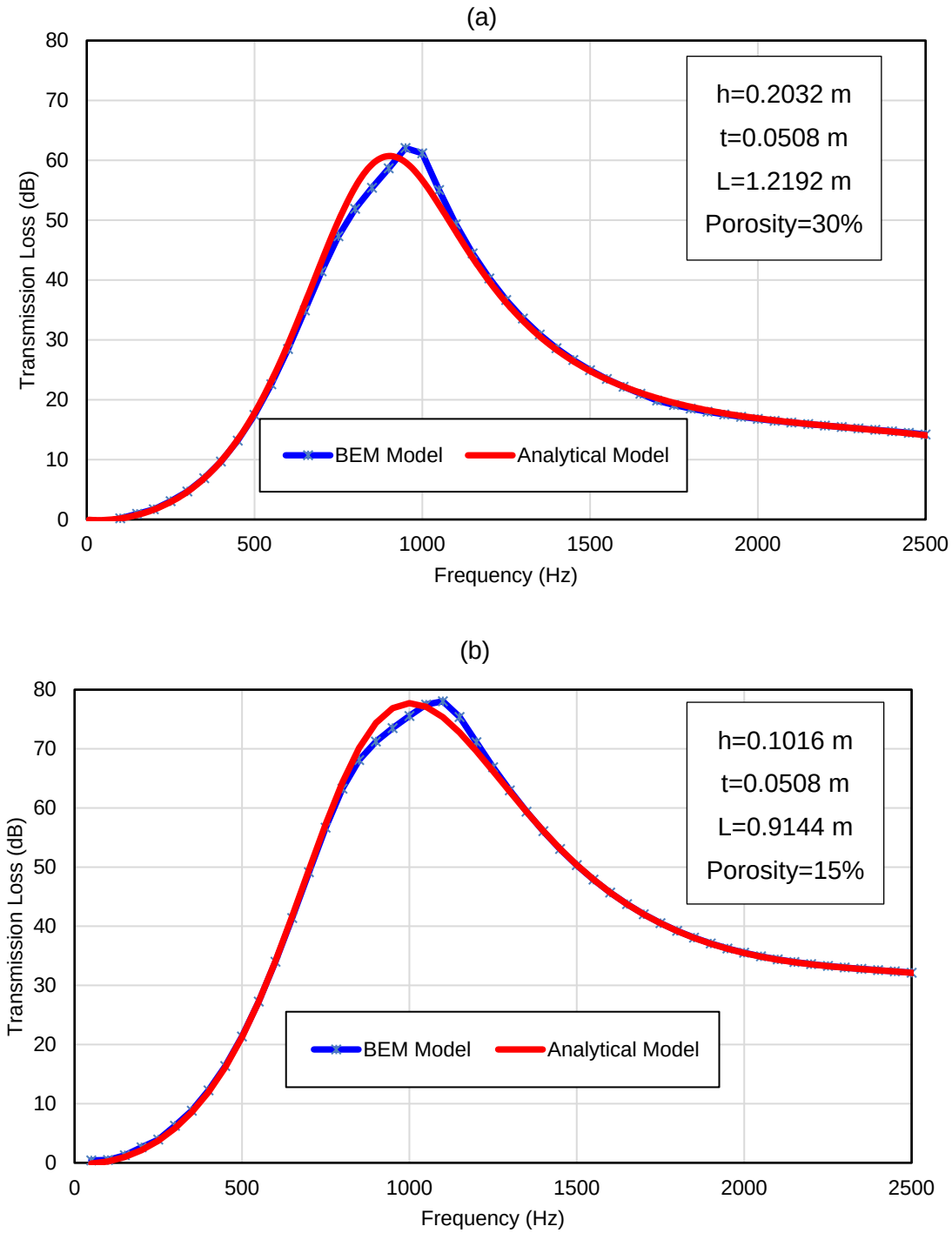

Figure 4.2: Comparisons between the local impedance analytical solutions and the corresponding BEM solutions.

Figure 4.3 compares the bulk-reacting analytical solutions to the corresponding BEM solutions for two other designs. The temperature is also set at room temperature. In both designs, the bulk-reacting analytical solutions compare favorably with the corresponding BEM solutions.

(a)

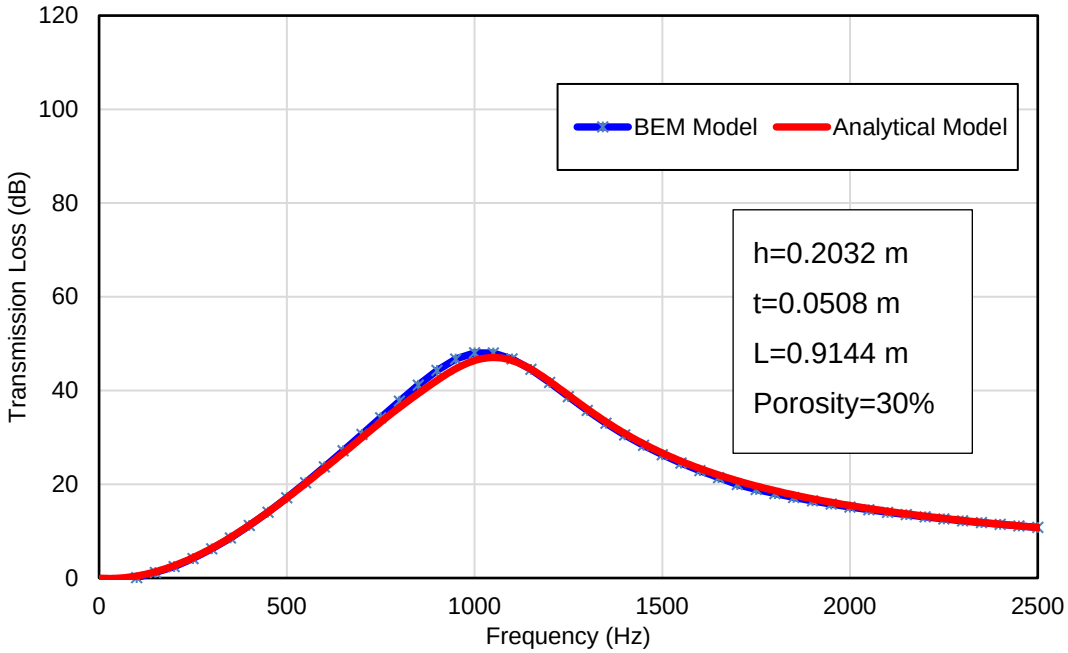

(b)

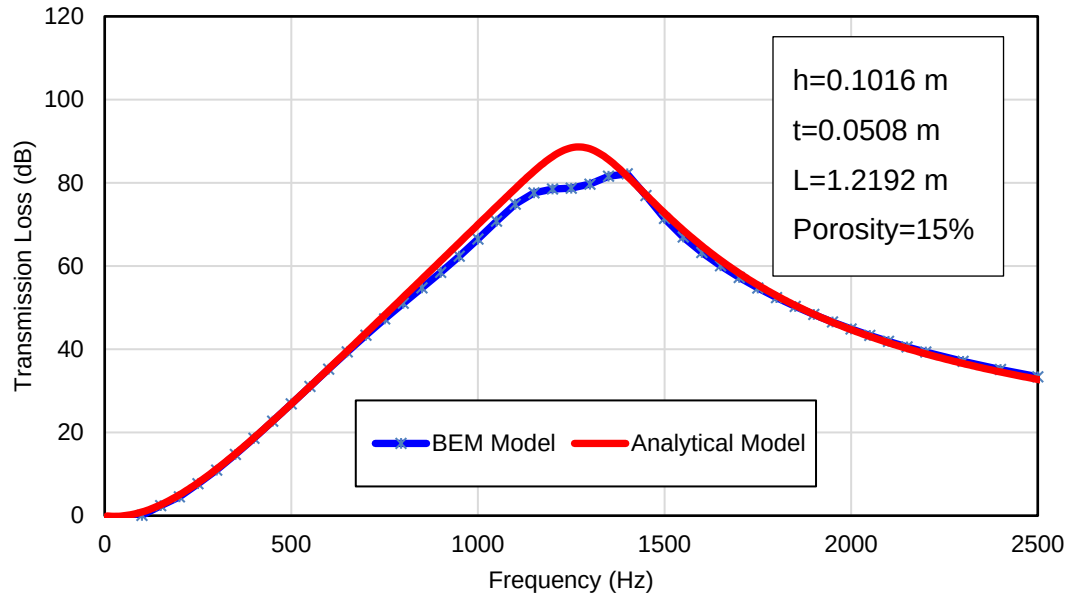

Figure 4.3 : Comparisons between the bulk-reacting analytical solutions and the corresponding BEM solutions.

In Figure 4.4, the locally reacting and bulk-reacting analytical solutions are compared against each other for several different designs. Figure 4.4 (a) and Figure 4.4 (b) compare the models for two different spacing values, Figures 4.4 (a) and Figure 4.4 (c) are for two different flow resistivity values, and Figures 4.4 (a) and Figure 4.4 (d) are for two different lining thickness values. It is noticed that there are some differences between the locally reacting and bulk-reacting solutions. In general, if the lining has thicker or denser sound absorbing material, the differences between these two approaches are less noticeable.

(a)

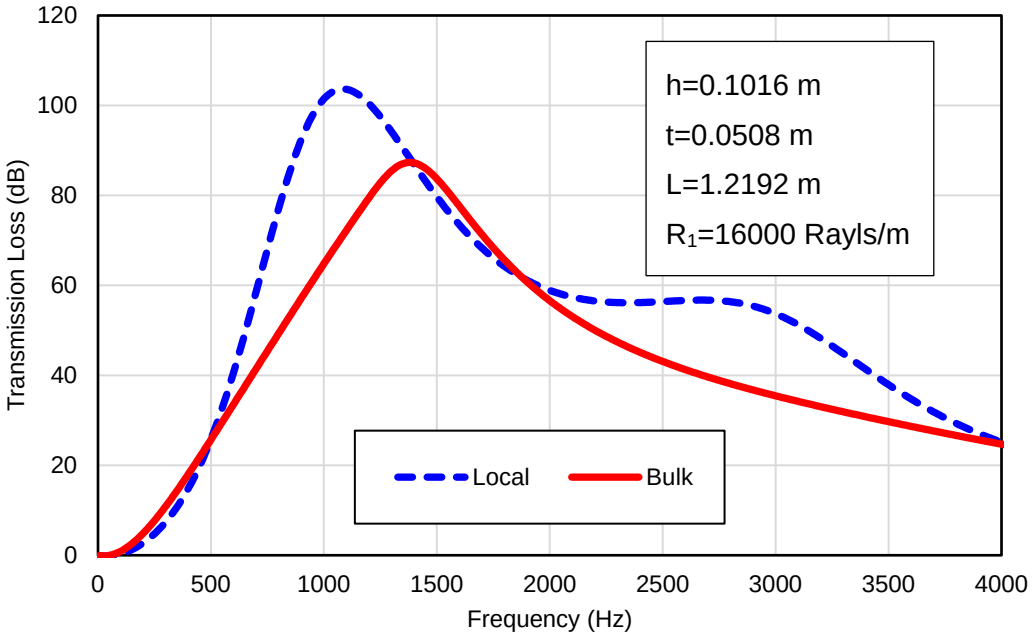
h=0.1016 m
t=0.0508 m
L=1.2192 m
R1=16000 Rayls/m
Local
Bulk
Transmission Loss (dB)
Frequency (Hz)
0
20
40
60
80
100
120
0
500
1000
1500
2000
2500
3000
3500
4000

(b)

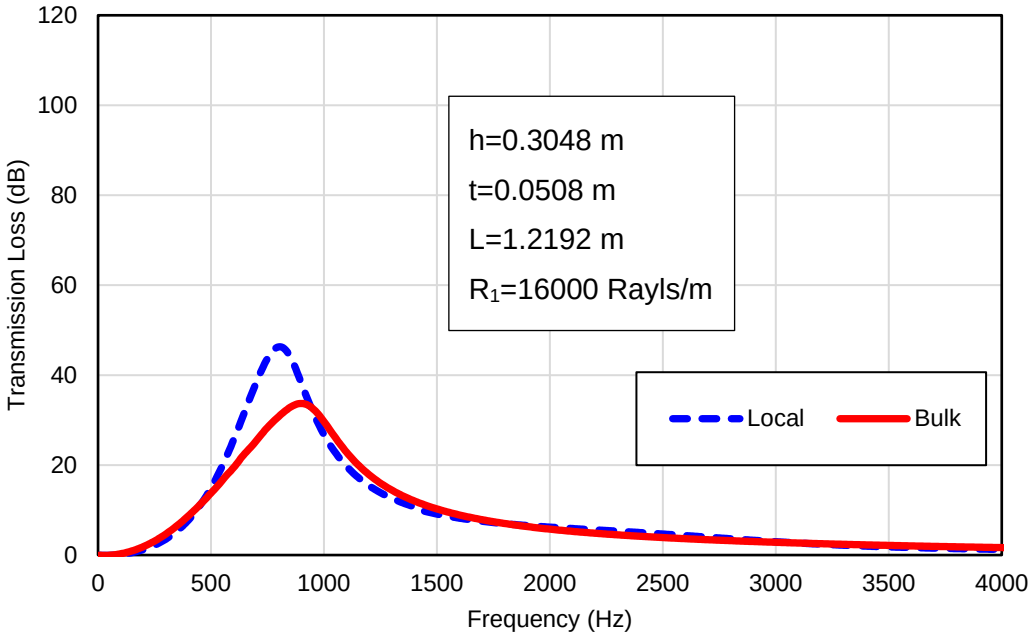
h=0.3048 m
t=0.0508 m
L=1.2192 m
R1=16000 Rayls/m
Local
Bulk
Transmission Loss (dB)
Frequency (Hz)
0
20
40
60
80
100
120
0
500
1000
1500
2000
2500
3000
3500
4000

(c)

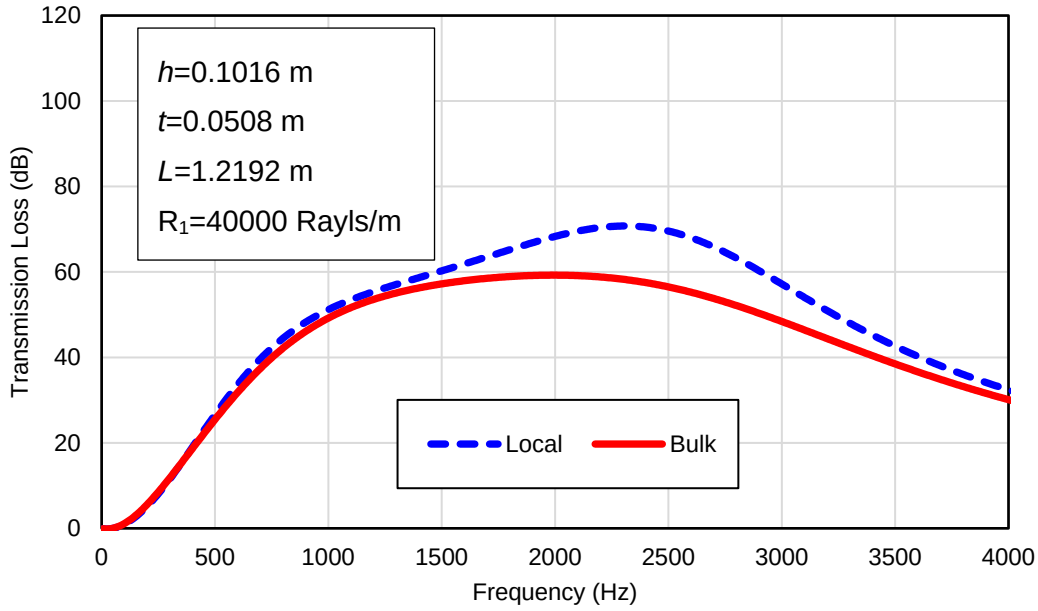

(d)

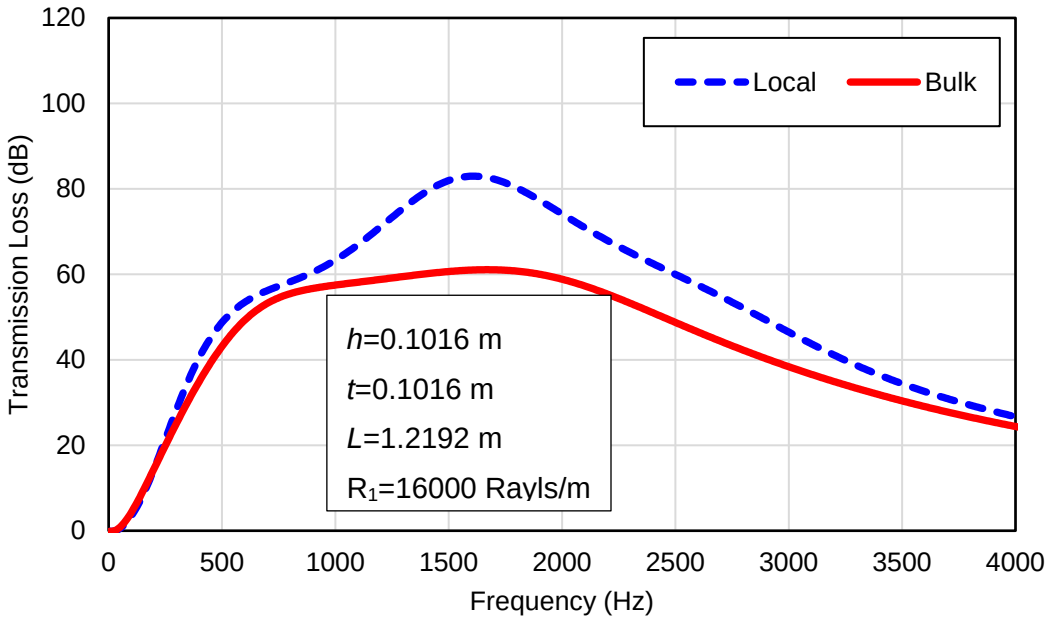

Figure 4.4: Comparisons between the locally reacting and the bulk-reacting analytical solutions.

4.2 Rectangular Ducts Lined on All Four Sides

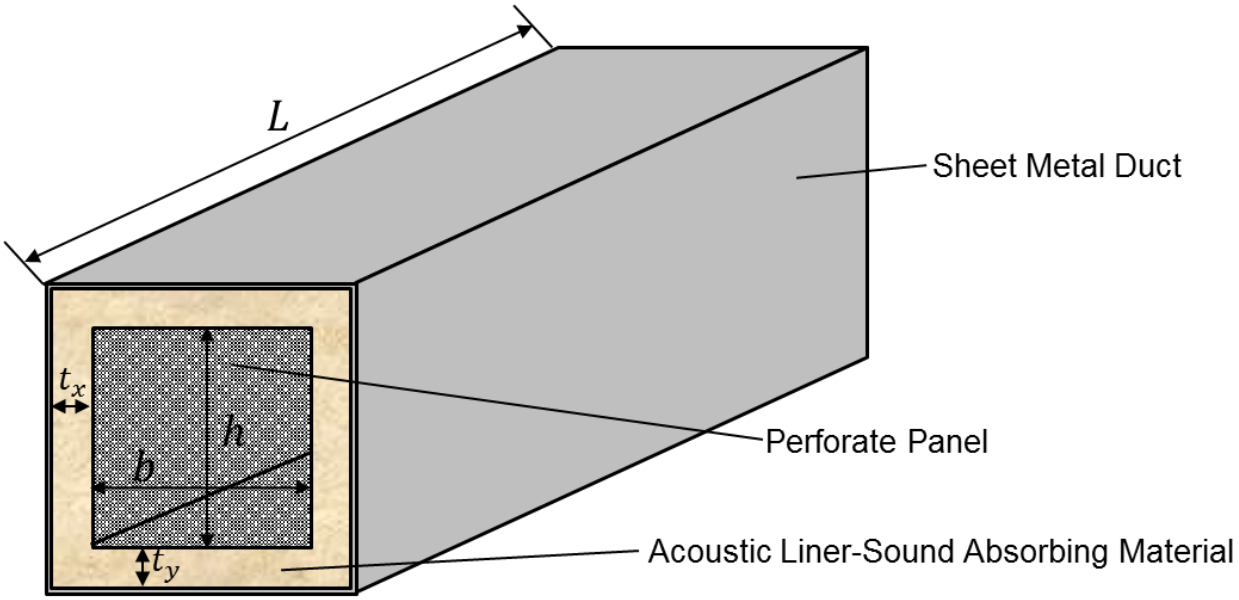

Figure 4.5 Geometry of a typical rectangular duct lined on all four sides

Figure 4.5 shows the geometry of a typical rectangular duct lined on all four sides. Figures 4.6 compares the bulk-reacting analytical solution of test case 1 to the corresponding BEM solution, and the dimensions are shown in the plot. Figure 4.7 shows the comparison for another design, with dimensions shown in the plot. As shown in both figures, the bulk reacting analytical solutions compares fairly well with the corresponding BEM solutions.

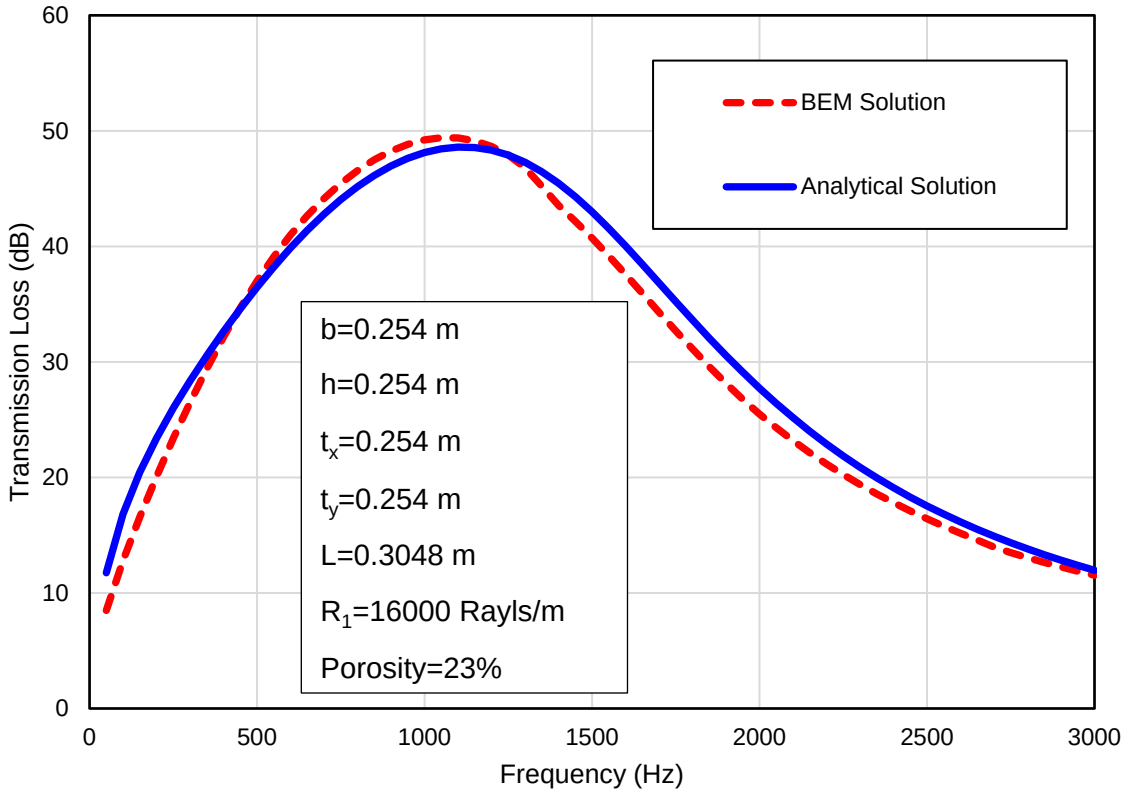

Figure 4.6 Comparison between the Bulk-Reacting Analytical Solution and the BEM Solution

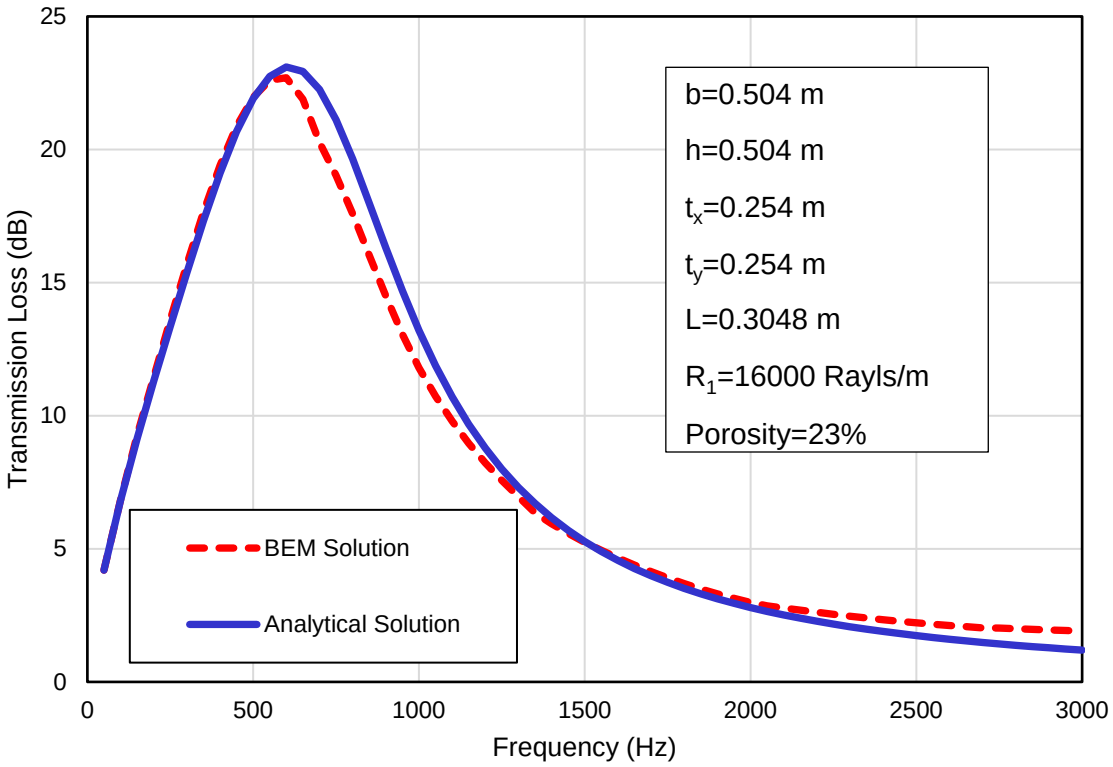

Figure 4.7 Comparison between the Bulk-Reacting Analytical Solution and the BEM Solution

4.3 Circular Duct

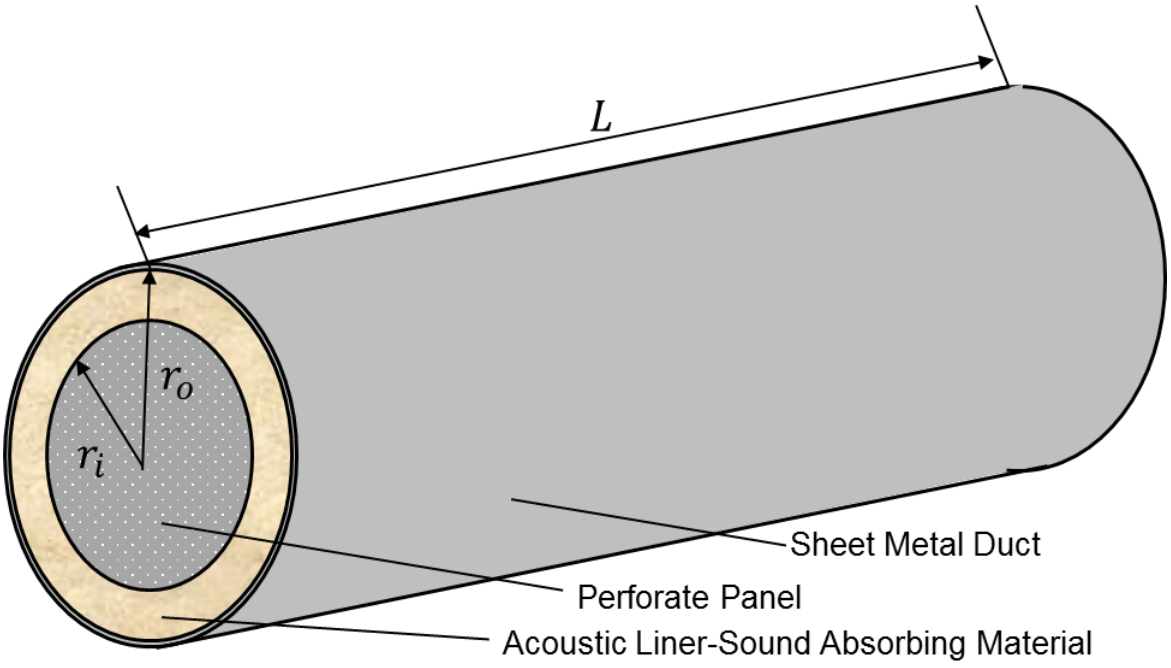

Figure 4.8 Geometry of a typical circular lined duct

Figure 4.8 shows the geometry of a typical circular lined duct. Test case 1 simulated a circular lined duct with dimensions shown in the plot. The result was shown in Figure 4.9. As is shown in the plot, the bulk reacting analytical solution compares with the BEM solution very well. The analytical result provides a very accurate solution in the low to middle frequency range, though some disagreement shows up at the high frequency range.

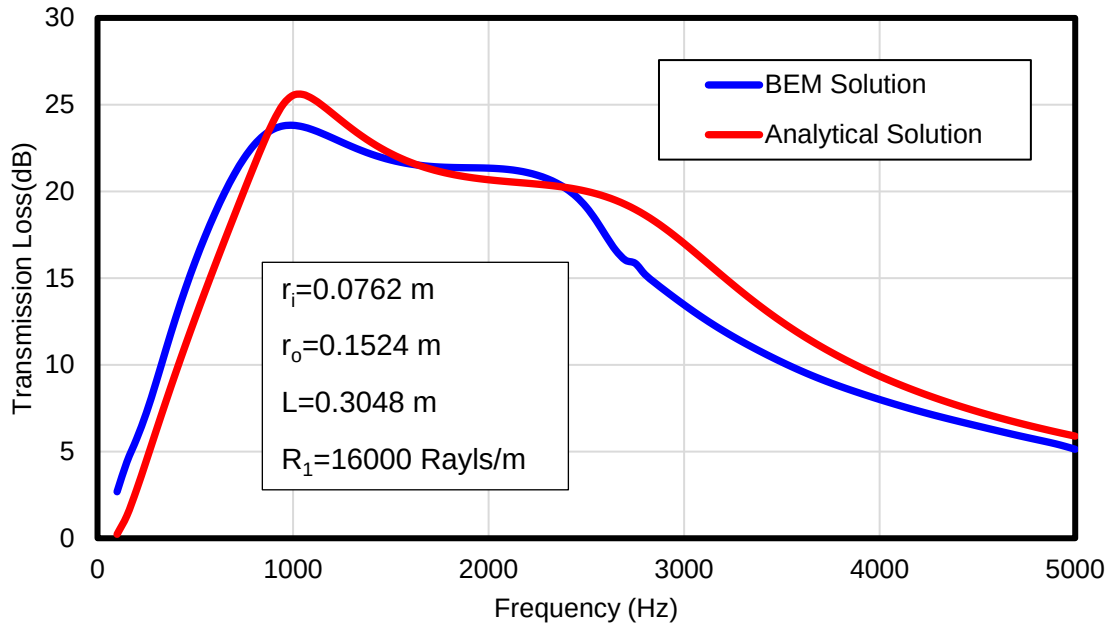

Figure 4.9 Comparison of Bulk Reacting Analytical Solution with BEM Solution of Test Case 1

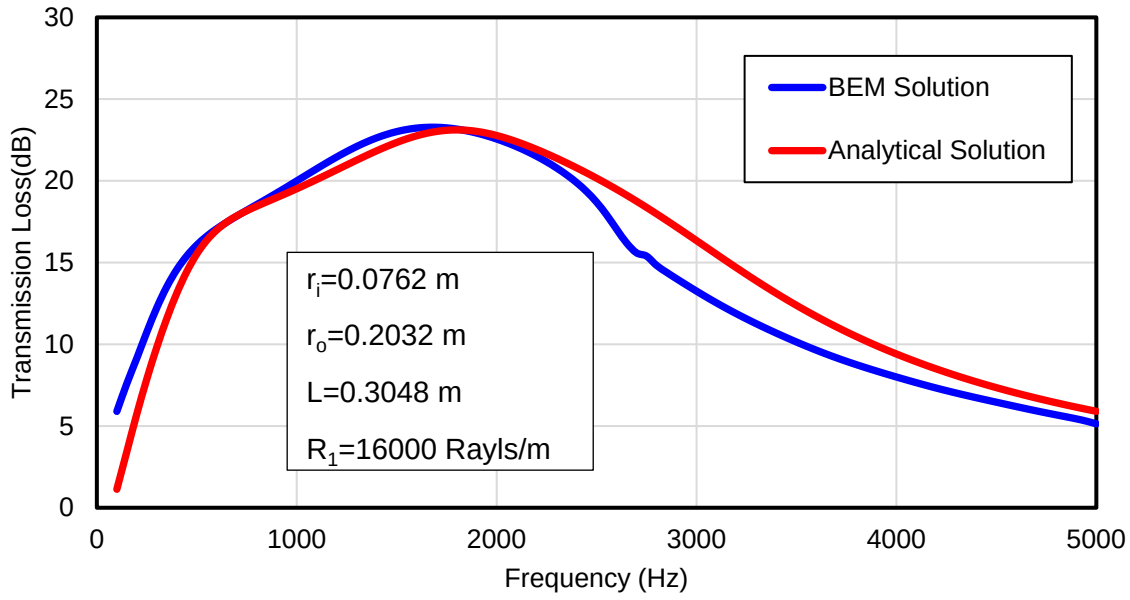

Figure 4.10 Comparison of Bulk Reacting Analytical Solution with BEM Solution of Test Case 2

Another design has also been performed. Test case 2 is a circular lined duct with thicker sound absorbing liner. The result was shown in Figure 4.10. As can be seen from the plot, the bulk reacting analytical solution agrees well with BEM simulation. Therefore, results demonstrate that the bulk reacting analytical model provides acceptably predicts the duct attenuation.

Results of using different types of empirical formulas for perforates are also generated as well, which is shown in Figure 4.11. The simulation of this test case is based on a circular lined duct with a micro-perforated panel tube between the air channel and sound absorbing material. The porosity of the perforated panel is 1%.

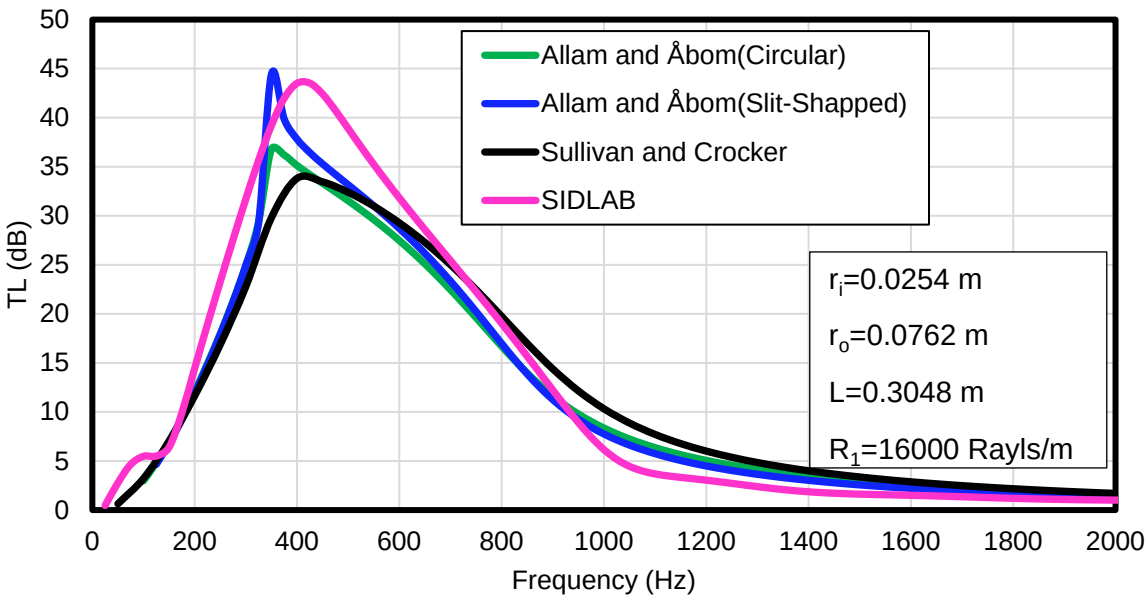

Figure 4.11 Comparisons of Different Empirical Formulas for Micro-perforated Panels

As can be seen from the plot, different empirical equations work differently with micro-perforated panels. It was proved by Allam and Åbom that while dealing with problems with Micro-perforated tubes inside, the traditional empirical equations will be less accurate. The equations developed by Allam and Åbom was recommended.

CHAPTER 5 CONCLUSIONS AND RECOMMENDATIONS FOR FUTURE RESEARCH

5.1 Conclusions

Two-dimensional and three-dimensional bulk-reacting analytical methods for rectangular and circular lined ducts are presented. Each method is validated by comparing to the corresponding BEM solution. It has also been demonstrated that there are differences between the bulk-reacting and locally reacting models. The developed analytical models will be useful as a means to rapidly assess the acoustical performance of lined ducts in HVAC systems and parallel-baffle silencers commonly used in gas turbines.

A BEM model for a full 3D parallel-baffle silencer is also constructed to compare to the simplified 2D locally reacting and bulk-reacting solutions. It is found that the simplified 2D bulk-reacting model can produce a decent solution very close to the full 3D parallel-baffle silencer BEM solution.

The presented work provides the bulk-reacting analytical solutions for different lined ducts. The proposed method shows more accurate solutions when compared to the local impedance method. Results of the test cases have demonstrated that this bulk-reacting analytical method can provide a rapid and accurate alternative to the full BEM solution for lined ducts.

5.2 Recommendations for future research

The following are the recommendations for future research:

1. Small-scale experiments should be performed in the lab for further validation, since full scale on-site measurements are difficult.
2. Temperature correction factor on the material properties should be investigated.

3. The nonlinear solver used in this thesis to solve the characteristic equations can be refined to avoid failing to find the correct first-mode root in rare and extreme designs, such as very thin liners in a large cross section. General guidelines should also be developed to let users know the dimensional limits for which the solver will be able to converge.

4. It would be beneficial to develop a GUI program for user-friendly applications.

5. More research can be performed to study the effects of using different sound absorbing linings in parallel-baffle silencers and rectangular lined ducts.

6. Normalized design curves should be generated as quick design references.

References

[1] Peat, K.S. and Rathi, K.L., A finite element analysis of the convected acoustic wave motion in dissipative silencers. Journal of Sound and Vibration 184 (1995) 529-545.

[2] Kirby, R., Transmission loss predictions for dissipative silencers of arbitrary cross section in the presence of mean flow. The Journal of the Acoustical Society of America, 114(1), pp.200-209 (2003)

[3] Astley, R.J., Cummings, A. and Sormaz, N., 1991. A finite element scheme for acoustic propagation in flexible-walled ducts with bulk-reacting liners, and comparison with experiment. Journal of Sound and Vibration, 150(1), pp.119-138.

[4] Wu, T. W., Cheng, C. Y. R. and Zhang, P., A direct mixed-body boundary element method for packed silencers, J. Acoust. Soc. Am., 111, 2566-2572 (2002).

[5] Wang, P. and Wu, T.W., 2016. Impedance-to-scattering matrix method for large silencer analysis using direct collocation. *Engineering Analysis with Boundary Elements*, *73*, pp.191-199.

[6] Morse, P.M., 1939. The transmission of sound inside pipes. The Journal of the Acoustical Society of America, 11(2), pp.205-210.

[7] K. Ingard, Notes on Sound Absorption Technology, Noise Control Foundation, New York, 1994.

[8] Scott, R.A., 1946. The propagation of sound between walls of porous material. Proceedings of the Physical Society, 58(4), p.358.

[9] Brittain, C.P., Maguire, C.R., Scott, R.A. and King, A.J., 1948. Attenuation of sound in lined air ducts. Engineering, 165, pp.97-98.

[10] King, A.J., 1958. Attenuation of sound in lined air ducts. The Journal of the Acoustical Society of America, 30(6), pp.505-507.

[11] Utsuno, H., Tanaka, T., Fujikawa, T. and Seybert, A.F., 1989. Transfer function method for measuring characteristic impedance and propagation constant of porous materials. The Journal of the Acoustical Society of America, 86(2), pp.637-643.

[12] Tao, Z., Herrin, D.W. and Seybert, A.F., 2003. Measuring bulk properties of sound-absorbing materials using the two-source method (No. 2003-01-1586). SAE Technical Paper.

[13] Munjal, M.L. and Doige, A.G., 1990. Theory of a two source-location method for direct experimental evaluation of the four-pole parameters of an aeroacoustic element. Journal of Sound and Vibration, 141(2), pp.323-333.

[14] Bernek, L.L. and Vér, I.L. eds., 2006. Noise and vibration control engineering: principles and applications. Wiley.

[15] Delany, M.E. and Bazley, E.N., 1970. Acoustical properties of fibrous absorbent materials. Applied acoustics, 3(2), pp.105-116.

[16] Miki, Y., 1990. Acoustical properties of porous materials-Modifications of Delany-Bazley models. Journal of the Acoustical Society of Japan (E), 11(1), pp.19-24.

[17] Attenborough, K., 1982. Acoustical characteristics of porous materials. Physics reports, 82(3), pp.179-227.

[18] Sullivan, J. W., Crocker, M., “Analysis of Concentric-tube Resonators Having Unpartitioned Cavities”, J Acoust Soc Am, 64(1), 207-215 (1978).

[19] Sullivan, J.W., 1979. A method for modeling perforated tube muffler components. I. Theory. The Journal of the Acoustical Society of America, 66(3), pp.772-778.

[20] Sullivan JW. A method for modeling perforated tube muffler components. II. Applications. The Journal of the Acoustical Society of America. 1979 Sep;66(3):779-88.

[21] Coelho, J.B., 1984. Modeling of cavity backed perforate liners in flow ducts. In Proceedings of 1984 Nelson Acoustics Conference.

[22] Nocke, C., Ke, L.I.U. and Dab-You, M.A.A., 2000. Statistical absorption coefficient of microperforated Absorbers. *Chinese Journal of Acoustics*.

[23] Allam, S. and Åbom, M., 2011. A new type of muffler based on microperforated tubes. Journal of Vibration and Acoustics, 133(3), p.031005.

[24] Selamet, A., Xu, M.B., Lee, I.J. and Huff, N.T., 2004. Analytical approach for sound attenuation in perforated dissipative silencers. The Journal of the Acoustical Society of America, 115(5), pp.2091-2099.

[25] ASTM E2611-09, *Standard Test Method for Measurement of Normal Incidence Sound Transmission of Acoustical Materials Based on the Transfer Matrix Method*, ASTM International, West Conshohocken, PA, 2009, www.astm.org

[26] Bies, D.A. and Hansen, C.H., 2009. *Engineering noise control: theory and practice*. CRC press.

[27] Kinsler, L.E., Frey, A.R., Coppens, A.B. and Sanders, J.V., 1999. Fundamentals of acoustics. *Fundamentals of Acoustics, 4th Edition, by Lawrence E. Kinsler, Austin R. Frey, Alan B. Coppens, James V. Sanders, pp. 560. ISBN 0-471-84789-5. Wiley-VCH, December 1999.*, p.560.

[28] Beyer, W.H., CRC Standard Mathematical Tables, 28th edn., 1987.

[29] Munjal, M.L., 2014. *Acoustics of Ducts and Mufflers*, 2nd Edition. John Wiley & Sons.

[30] Li, J., Wang, P., Wu, T. and Herrin, D., 2016, June. Analytical and Boundary Element Solutions of Bulk-Reacting Lined Ducts and Parallel-Baffle Silencers. In *INTER-NOISE and NOISE-CON Congress and Conference Proceedings* (Vol. 252, No. 2, pp. 720-727). Institute of Noise Control Engineering.

[31] Wang, P., Li, J. and Wu, T.W., 2015. Numerical Determination of Transfer Impedance for Perforates. *SAE International Journal of Passenger Cars-Mechanical Systems*, *8*(2015-01-2312), pp.1003-1008.

[32] Maling Jr, G.C. and Lang, W.W., 1973. Theory into practice: A physicist's helpful view of noise phenomena. *Noise Control Engineering*, *1*(1), pp.46-59.

[33] Chen, H. and Herrin, D.W., 2015. A Parametric Investigation of Louvered Terminations for Rectangular Ducts. *SAE International Journal of Passenger Cars-Mechanical Systems*, *8*(2015-01-2356), pp.1137-1141.

[34] Ingard, K.U. and Maling, G.C., 1974. Physical principles of noise reduction- Energy considerations, noise reducing elements, and sound absorbing materials. *Noise Control Engineering*, *2*, pp.81-92.

[35] Kirby, R. and Cummings, A., 1999. Prediction of the bulk acoustic properties of fibrous materials at low frequencies. *Applied Acoustics*, *56*(2), pp.101-125.

[36] Munjal, M.L., Rao, K.N. and Sahasrabudhe, A.D., 1987. Aeroacoustic analysis of perforated muffler components. *Journal of Sound and Vibration*, *114*(2), pp.173-188.

[37] Wang, P., Zhou, L. and Wu, T.W., 2017. Comparison of an integral and a collocation based impedance-to-scattering matrix methods for large silencers analysis. *The Journal of the Acoustical Society of America, 141(5)*, pp.3615-3615.

VITA

Jundong Li was born in Dalian, China in 1989. He received the degree of Bachelor of Science in Mechanical Engineering from the University of Kentucky in 2014 with Hornor. He received the degree of Bachelor of Engineering in Measuring and Control Technology and Instrumentation from China University of Mining and Technology at the meantime. In August 2014, he continued his study at the Department of Mechanical Engineering at the University of Kentucky and enrolled in graduate school. During his three years graduate studies at University of Kentucky, he published two NOISE-CON conference paper and one SAE journal paper as second author and was awarded Michiko So Finegold Award by Institute of Noise Control Engineering (INCE). He joined Cummins Inc., as a full time Acoustics Engineer since March 2017.

Jundong Li